# A Comprehensive Approach to Battery Management System Incorporating Dynamic Power Limiting with Thermal Management Algorithm

AFSANUL HAQUE

SUPERVISORS
Mohan Lal Kolhe, UiA
Souman Rudra, UiA
Nur Mohammad, CUET

**University of Agder, [2023]**
Faculty of Engineering and Science
Department of Engineering Sciences

## Abstract

This study critically presents the model of a Battery Management System (BMS) for monitoring and controlling battery parameters in various applications. The presented model allows for comprehensive monitoring and analysis of critical battery metrics such as State of Charge (SOC), charging, discharging, and voltage. By developing and testing the model prior to hardware implementation, significant advantages including time and cost savings, as well as error identification, are realized. The BMS serves as a crucial component in these applications, ensuring efficient battery utilization, optimizing performance, and enhancing system safety.

Through the developed model, advanced algorithms and control strategies can be tested and fine-tuned to achieve optimal battery management. This iterative process helps overcome challenges and limitations associated with battery systems, leading to improved energy efficiency, extended battery life, and enhanced overall system performance. However, future research and development efforts are warranted to further enhance the simulation model's accuracy and responsiveness. Integration of real-time data acquisition and advanced control algorithms can facilitate more precise and adaptive battery management. Additionally, addressing limitations such as temperature effects, aging, and environmental variations will contribute to the continued advancement of BMS technology.

In conclusion, the design and model of the BMS presented in this study critically contribute to the ongoing progress in battery technology. By enabling comprehensive monitoring and control, the BMS facilitates the widespread adoption of battery-powered systems, supporting energy efficiency and sustainability in various industries and sectors.

## Abstrakt

Denne studien presenterer en kritisk modell av et batteristyringssystem (BMS) som overvåking og kontrollerer batteriparametere i ulike applikasjoner. Den presenterte modellen gir muligheten for omfattende overvåking og analyse av kritiske batterimålinger som State of Charge (SOC), lading, utlading og spenning. Ved å utvikle og teste modellen før maskinvareimplementering, oppnås betydelige fordeler, inkludert tids- og kostnadsbesparelser, samt feilidentifikasjon. BMS fungerer som en avgjørende komponent i disse applikasjonene, og sikrer effektiv bruk av batteriet, optimal ytelse og forbedret systemsikkerhet.

Gjennom den utviklede modellen kan avanserte algoritmer og kontrollstrategier testes og finjusteres for å oppnå optimal batteristyring. Denne iterative prosessen bidrar til å overvinne utfordringer og begrensninger knyttet til batterisystemer, noe som fører til forbedret energieffektivitet, forlenget batterilevetid og forbedret generell systemytelse. Imidlertid er fremtidig forsknings- og utviklingsinnsats berettiget for å ytterligere forbedre simuleringsmodellens nøyaktighet og respons. Integrering av sanntids datainnsamling og avanserte kontrollalgoritmer kan bodra til mer presis og adaptiv batterihåndtering. I tillegg vil adressering av begrensninger som temperatureffekter, aldring og miljøvariasjoner bidra til den fortsatte utviklingen av BMS-teknologi.

Avslutningsvis bidrar designen og modellen til BMS presentert i denne studien kritisk måte til den pågående fremgangen innen batteriteknologi. Ved å muliggjøre omfattende overvåking og kontroll, letter BMS den utbredte bruken av batteridrevne systemer, og støtter energieffektivitet og bærekraft i ulike bransjer og sektorer.

## Preface

In this dissertation, I, Afsanul Haque, as a participant in the NORPART-2021/10355 (CARE) project and an exchange student pursuing a Master's degree, present the culmination of my academic journey. This MSc thesis credits are going to be used in my CUET post-graduate degree completion. This groundbreaking research endeavor has expanded my horizons and fortified my proficiency in the subject matter. The genesis of this thesis is rooted in my educational foundation and fervor for the topic, which can be traced back to my previous academic endeavors. The impetus for undertaking this study stems from my desire to explore the complexities of my chosen field and contribute to its advancement. This thesis targets individuals with an interest in the subject, encompassing scholars, specialists, and practitioners. The aim is to furnish innovative insights and perspectives, thereby stimulating further inquiry and progress in the field.

I extend my heartfelt gratitude to Prof. Dr. Mohan Lal Kolhe and Prof. Dr. Souman Rudra from the University of Agder (UiA), Norway, as well as Prof. Dr. Nur Mohammad from the Chittagong University of Engineering & Technology (CUET), Bangladesh, for their unwavering support and invaluable counsel throughout this journey. Their expertise and mentorship have been instrumental in shaping the trajectory of this dissertation. Moreover, I am profoundly appreciative of Dr. Rambabu Kandepu from Corvus Energy for his remarkable commitment, tenacity, and willingness to share his vast knowledge in this domain.

Additionally, I wish to convey my thanks to the NORPART-2021/10355 (CARE) project for providing me with an extraordinary educational opportunity and fostering cross-cultural exchange. I also express my earnest gratitude to my family, friends, and loved ones for their unyielding support during this challenging expedition.

Afsanul Haque
University of Agder (UiA), Norway
& CUET, Bangladesh.

## Individual/group Mandatory Declaration

The individual student or group of students is responsible for the use of legal tools, guidelines for using these and rules on source usage. The statement will make the students aware of their responsibilities and the consequences of cheating. Missing statement does not release students from their responsibility.

| | | |
|---|---|---|
| 1. | I/We hereby declare that my/our report is my/our own work and that I/We have not used any other sources or have received any other help than mentioned in the thesis. | ☒ |
| 2. | I/we further declare that this thesis:<br>- has not been used for another exam at another department/university/university college in Norway or abroad;<br>- does not refer to the work of others without it being stated;<br>- does not refer to own previous work without it being stated;<br>- have all the references given in the literature list;<br>- is not a copy, duplicate or copy of another's work or manuscript. | ☒ |
| 3. | I/we am/are aware that violation of the above is regarded as cheating and may result in cancellation of exams and exclusion from universities and colleges in Norway, see Universitets- og høgskoleloven §§4-7 og 4-8 og Forskrift om eksamen §§ 31. | ☒ |
| 4. | I/we am/are aware that all submitted theses may be checked for plagiarism. | ☒ |
| 5. | I/we am/are aware that the University of Agder will deal with all cases where there is suspicion of cheating according to the university's guidelines for dealing with cases of cheating. | ☒ |
| 6. | I/we have incorporated the rules and guidelines in the use of sources and references on the library's web pages. | ☒ |

## Publishing Agreement

Authorization for electronic publishing of the thesis.

Author(s) have copyrights of the thesis. This means, among other things, the exclusive right to make the work available to the general public (Åndsverkloven. §2).

All theses that fulfill the criteria will be registered and published in Brage Aura and on UiA's web pages with author's approval.

Theses that are not public or are confidential will not be published.

I hereby give the University of Agder a free right to

make the task available for electronic publishing: ☒JA ☐NEI

Is the thesis confidential? ☐JA ☒NEI

(confidential agreement must be completed and signed by the Head of the Department)

- If yes:

Can the thesis be published when the confidentiality period is over? ☐JA ☐NEI

Is the task except for public disclosure? ☐JA ☒NEI

(contains confidential information. see Offl. §13/Fvl. §13)

# Table of Contents

## List of Figures

# List of Tables

## Notation

I→ Current (A)

V→Voltage (V)

U→Open circuit potential (V)

R→Resistance (ohm)

$Q_g$→Heat generation (J)

$Q_d$→ Heat rejection (J)

$R_e$→ Equivalent internal resistance (ohm)

T→ Temperature (K)

E→ Energy (J)

Tf→ Fluid temperature (K)

Ta→ Ambient temperature (K)

h→heat transfer coefficient ($W/m^2.K$)

A→Area for heat transfer (m2)

$\varepsilon$→Emission ratio

$\sigma$→Steffan-Boltzman constant ($W/m^2.K^4$)

# Abbreviations

# 1. Introduction

## 1.1. Background

The severity of the energy and environmental crises could be considerably decreased with the use of renewable energy sources. However, because of the intermittent nature of these renewable energy sources, energy storage systems have gained traction in a diverse range of applications. Therefore, modern energy storage technologies are needed to integrate renewable energy production into the global energy system. In terms of energy and power densities, cycle life, and self-discharge rate, lithium batteries outperform other chemistries, and they are the cutting edge of these storage technologies [1]. When they charge and discharge, a substantial amount of heat is produced, which raises the temperature [2]. Therefore, most batteries should ideally operate at an ideal average temperature with a relatively small differential range [3] [4]. A power performance map that displays the useable power of batteries in relation to the operational circumstances (such as temperature, voltage, and capacity) will serve as a roadmap for utilizing the batteries to their maximum potential while preserving safety [5]. As figure 1 depicts, Battery Management System (BMS) serves the purpose of reporting the charge and discharge power to and available from the battery, among other functions. Several power versions may be needed to satisfy the supervisory controller, depending on the control's time frame. If high temperature is the limiting factor, the thermal system's capacity to tolerate the cells' rate of heat generation as a function of power may be the limiting factor for continuous power [6].

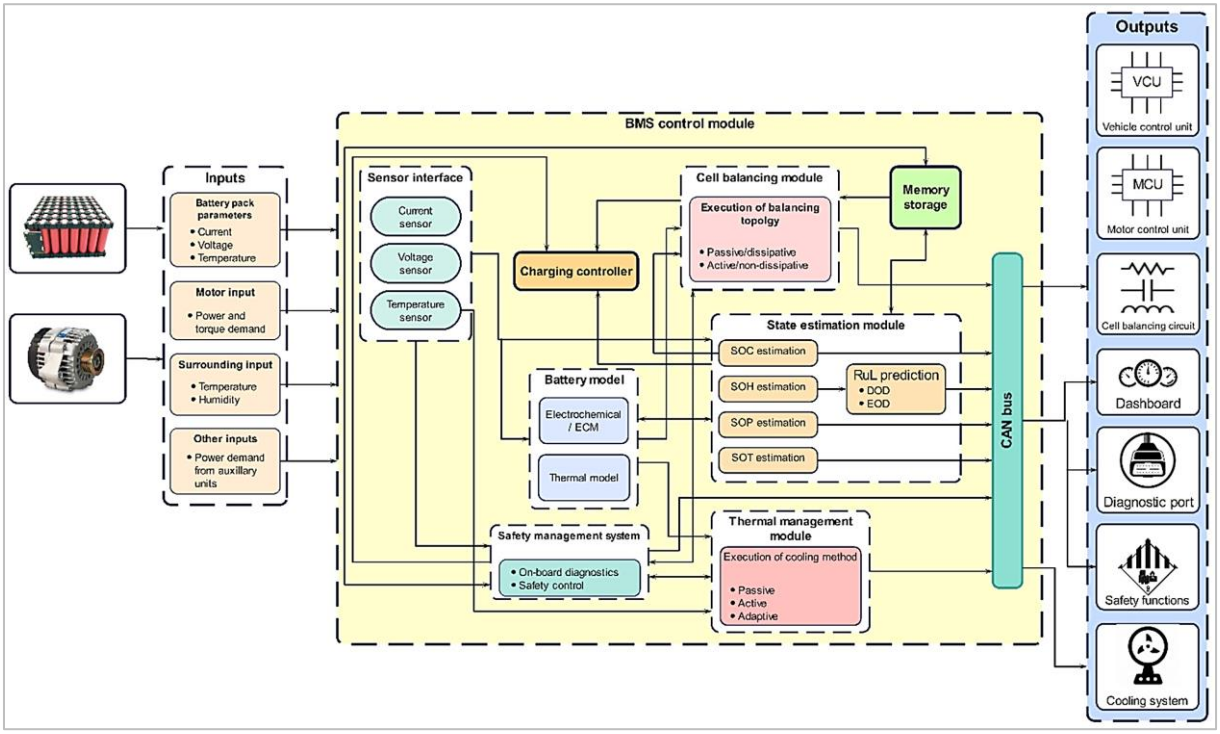


*Figure 1: Structure of Battery Management System [7]*

## 1.2. Research Questions

The primary objective of this thesis is to investigate, develop, and evaluate novel techniques for dynamic power limit management in Battery Management Systems (BMS) to improve battery performance, safety, and lifespan. To achieve this objective, the following research questions have been defined:

1) What is the influence of temperature and state of charge (SOC) on heat transfer phenomena in a battery system?
2) What mathematical function can be utilized to quantify the accumulation of heat in a battery cell during both charge and discharge processes?
3) How to optimize the accumulated heat in the cell and what are the limits on that function?
4) How to generate current/power limits based on usage for different time periods into the future?
5) How can the developed dynamic power limit algorithms be integrated into existing BMS for various battery applications, such as EV, PV etc.?

## 1.3. Thesis definition

This thesis analyzes the thermal issues with Lithium-ion Battery to develop an algorithm for BMS to operate the battery within the prescribed temperature limit.

The objective of this thesis is to:

- Find the heat generation in the battery.
- Calculate the heat rejection from the battery.
- Compute the heat accumulation in the battery.
- Analyze to find an optimal solution to this heat accumulation with the all the limits.
- Simulate the developed algorithm.

## 1.4. Thesis Organization

This thesis focuses on developing and evaluating novel dynamic power limit algorithms for Battery Management Systems (BMS) to enhance battery performance, safety, and lifespan. **Chapter 2** represents the literature review of the existing study and approaches to the problem, the equations required to solve the identified problem. **Chapter 3** includes the research questions that are identified to answer in this thesis. The procedures that are followed to achieve the objective, including algorithm development, are represented in **Chapter 4. Chapter 5** explains the results in the light of theory and describes the discussion of the results. **Chapter 7** is the Conclusion which describes the summary of findings, contributions, and potential future work.

# 2. Battery Parameterization

## 2.1. Literature Review

Previously published literature has emphasized the challenge of determining the maximum power or speed capacity of Li-ion cells, without giving much consideration to the impact of temperature. The definition of State-of-Power (SOP) was initially established in reference number [8] as the proportion of obtainable energy to the standard energy of a battery. Most methods for predicting standard operating procedures (SOPs) utilize strategies that are based on the equivalent circuit model. These strategies are generally used in the field and have been supported by existing research [9] [10] [11]. In reference [12], they demonstrated how to estimate an SOP when faced with many limitations by using simplified resistor-capacitor (RC) models and methods based on an extended Kalman filter. In reference number [13], there was a semi-experimental design created for speed ability that relies on a modifiable factor. This variable can be adjusted according to the results obtained from evaluating a new cell's performance, and you can investigate the significance of various occurrences within the cell using a straightforward and understandable model.

In reference [14], a better technique utilizing the Thevenin representation was created to estimate the maximum power. The study mentioned in Reference [15] centered on limitations related to heat when operating at the highest power output, as well as limitations linked to the state of charge and voltage. Numerous studies provide the groundwork for estimating power delivery capacity, yet most of them are restricted by the utilization of simplified or empirical models. These models do not incorporate detailed temperature-related factors, which restrict their usefulness in various temperature conditions and pulse durations. Such limitations result in inaccuracy when assessing critical variables like voltage, state of charge and ultimately power. Inaccuracies in predicting power limits in colder temperatures can reach a maximum of 10% when utilizing current advanced models. This level of inaccuracy is unsatisfactory for ensuring a seamless customer experience [11].

## 2.2. Lithium-ion Batteries

Lithium exists in the positive electrode of lithium-ion batteries, and during charging and discharging, lithium ions flow from the positive electrode to the negative electrode through an electrolyte. Lithium-ion batteries have an advantage over other battery technologies due to their higher mass and volumetric energy densities. Since energy density is so important in the automotive industry, lithium-ion batteries are particularly appealing for this application. The four different form factors used to create lithium batteries are coin, cylindrical, prismatic, and pouch.

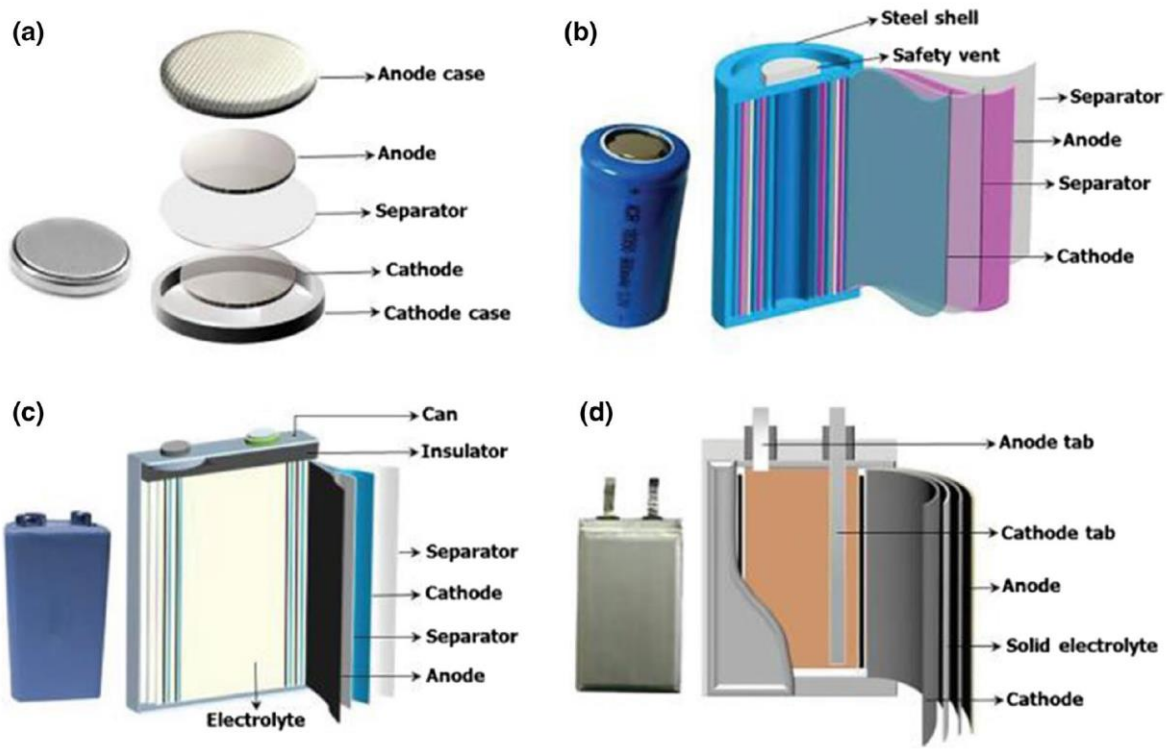


*Figure 2 Li-ion (a) Coin, (b) cylindrical, (c) prismatic, (d) pouch cell compositions. [16]*

Metallic lithium serves as the anode in lithium coin cell as shown in figure 2(a). Figure 2(b) depicts the layers are rolled and placed into a cylindrical container for cylindrical cells. The mechanical stability and simplicity of manufacture are advantages of this cell structure. Prismatic cell, in figure 2(c), is packaged to meet thinner design requirements. They are primarily present in electrical gadgets like mobile phones. Due to the removal of the metal cage and the ability to stack, pouch cells, in figure 2(d), have the most effective packaging.

Commercial lithium-ion batteries (LIBs) primarily utilize a carbon-based intercalation anode and a cathode composed of mixed lithium transition metal oxides or olivine compounds, such as $LiCoO_2$ (LCO), $LiNi_xCo_yMn_zO_2$ (NMC), NCA, $LiNi_xCo_yMn_zO_2$ (LMO), and $LiFePO_4$ (LFP) [17]. To achieve high energy/power density, cost reduction, longer lifetime, and safety, researchers are focusing on boosting the capacity, operating potentials, and cell voltage of the electrodes. This entails adopting new materials like silicon for more theoretical capacity [18], higher cell voltages [19], and solid-state electrolytes to enable quicker charging rates [20] and better safety [21].

## 2.3. Optimal Working Temperature

Although Li-ion performs well in hot environments, continuous heat exposure shortens its lifespan [22]. The best temperature range for Li-ion battery performance, according to the report [23], is between 15℃ and 35℃ Celsius as described in figure 3.

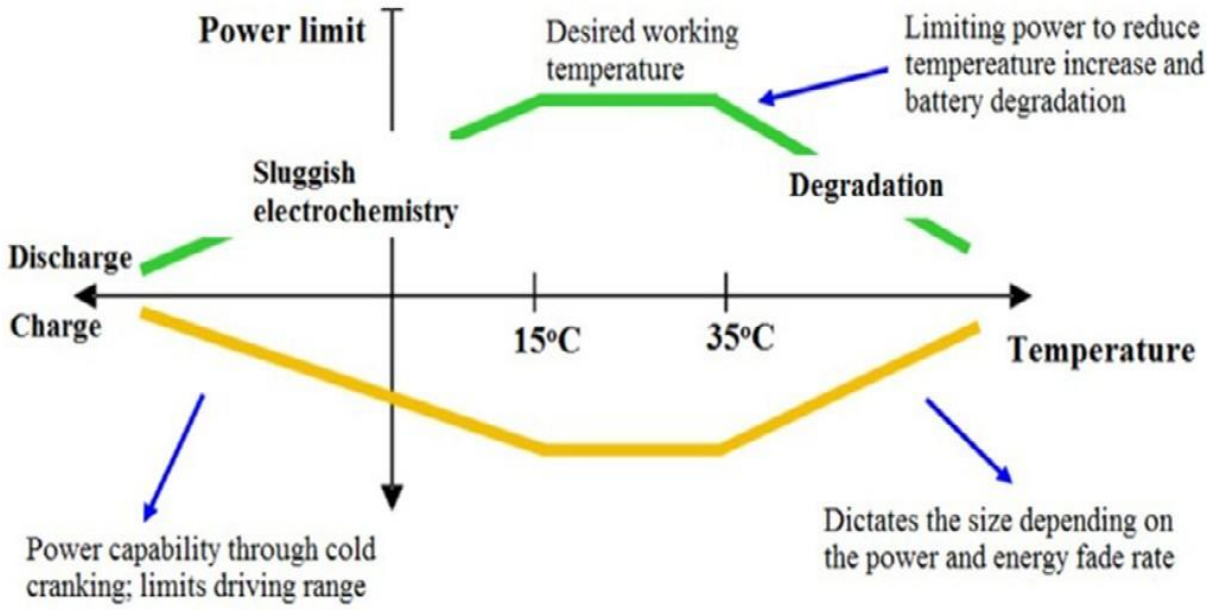


*Figure 3: Lithium-ion Battery optimal working temperature [22]*

## 2.4. Heat Generation

Three principal processes cause heat to be produced in LIBs: (a) Joule heating, also known as "ohmic" heating, which restricts the movement of electrons; (b) electrode reactions, which result from a charge transfer between the electrodes and electrolyte; and (c) entropic heating, which is caused by a modification in the arrangement of atoms within the crystal structure of the electrodes as a result of the intercalation and deintercalation of Li-ions [6] [24]. Other processes that contribute to the production of heat include the heat generated during mixing because of variations in the battery's concentration as the reaction progresses and the heat released during material phase changes [25].

The reaction in the Lithium Ion Battery is

$$LiCoO_2 + C_6 \leftrightarrows LiC_6 + CoO_2$$

Assuming a thermodynamic energy balance on a cell, Bernardi et al. [25] obtained the following formula for heat generation in LIBs which is used in the most literatures:

$$Q_g = I(U - V) - I(T\frac{dU}{dT}) \quad (2.1)$$

Where,

$Q_g$= Heat generation in the cell

I= Current, A (I>0 for discharge and I<0 for charge)

U= Open circuit potential, V

V= Voltage, V

T= Temperature, K

$I(U - V)$ = Heat Generation due to Cell polarization (Irreversible heat generation due to Joule heating)

$I\left(T\frac{dU}{dT}\right)$ = Reversible entropic heat, expressed as the potential derivative with respect to temperature.

For Simplification, in eq. (2.1), mixing and phase change terms are neglected [26].

Therefore, eq. (2.1) can be written as [26] [27]

$$Q_g = I^2 R_e - IT\left(\frac{dU}{dT}\right) \qquad (2.2)$$

Where, $R_e$ is the equivalent internal resistance (Ω). This is to be noted that the equation stated in eq. (2.2) presumes that the entire battery operates steadily at a uniform temperature and state of charge (SOC), typically applicable to smaller form factor batteries. Any fluctuations in temperature or SOC in different regions of the battery are disregarded. While the equations can provide an analytical projection of the total heat generation of the battery, it fails to factor in the specific temperature dispersion and localized heat concentration within the electrodes.

Here, for a 2.2 Ah LFP cell, $R_e$ can be represented in terms of T (in K) and estimated SOC (State-of-charge) [28]

$$R_e = 27.54 - 27.68exp\left(\frac{-1.91}{T}\right) + \left(\frac{223.71}{1+21.1\,SOC}\right) - \frac{225.06exp\left(\frac{-1.91}{T}\right)}{1+21.61\,SOC} \qquad (2.3)$$

Table 1: Expressions of Internal Electrical Resistance [28]

| Srl No. | Cell type | Expression or Value |
|---|---|---|
| 1 | LMO Cylindrical | $R_e = -0.0001T^3 + 0.0134T^2 - 0.5345T + 12.407$ |
| 2 | 2.2 Ah $LiFePO_4$ Cylindrical cell | $R_e = 27.54 - 27.68exp\left(\frac{-1.91}{T}\right) + \left(\frac{223.71}{1+21.1\,SOC}\right) - \frac{225.06exp\left(\frac{-1.91}{T}\right)}{1+21.61\,SOC}$ |
| 3 | SONY-US50G3 Cylindrical | $R_e = \begin{cases} 2.258 \times 10^{-6} SOC^{-0.3952}, & T = 293\ K \\ 1.857 \times 10^{-6} SOC^{-0.2787}, & T = 303\ K \\ 1.659 \times 10^{-6} SOC^{-0.1692}, & T = 313\ K \end{cases}$ |
| 4 | 1.25 Ah Sony 18650 Cylindrical | $R_e = f(DOD), 0.8 - 1.8$ |
| 5 | 20 Ah Lithium-Ion Polymer Battery | $R_{series} = 0.035 + 0.1562\exp(-24.74\,SOC)$<br>$R_{trans,s} = 0.04669 + 0.3208\exp(-29.14\,SOC)$<br>$R_{trans,l} = 0.04984 + 6.604\exp(155.2\,SOC)$ |
| 6 | 60 Ah Prismatic Battery | 1.61 mΩ (Charging), 0.937 mΩ (Discharging) |

The reversible entropic heat which is the second term in eq. (2.2) is a function of SOC and can be expressed as [28]

$$\frac{dU}{d\mathrm{T}} = 29.41SOC^6 - 54.18SOC^5 + 20.64SOC^4 + 8.4946SOC^3 - 5.4224SOC^2 + 1.0674SOC - 0.2057 \qquad (2.4)$$

## 2.5. Heat Rejection

Lithium-ion batteries (LIBs) have advantages over traditional batteries, but efficient thermal management systems are needed to increase their lifespan and reduce the possibility of thermal runaway due to heat buildup. Prior to their application, it is essential to solve the key issue of controlling the heat and temperature in LIBs. Heat has been dissipated and the temperature of LIBs has been controlled using a variety of thermal management technologies, including air cooling, and liquid cooling, Phase Change Materials (PCM), and heat pipes. Since they have several advantages and disadvantages over one another, it is still difficult for researchers and engineers to choose the best thermal management system for a certain LIB chemistry, nominal capacity, and intended application with specific charge and discharge rates (C-rates) or duty cycle. [28]

There are three methods by which heat can be conveyed: conduction, convection, and radiation, all of which are involved in the loss of heat within the cell. Initially, heat is conducted through the cell and reaches its outer boundary. Then, it is emitted into the surrounding environment or cooling media through processes of convection and radiation. In thermal management systems that rely on direct contact between batteries and coolant fluids, whether it be passive or active cooling, the transfer of heat from the cell boundary to the coolant is mainly due to convective and radiative processes, as conduction is generally not very effective during normal operations. [29]

Heat rejection or dissipation can be expressed as [30]

$$Q_d = hA\left(T - T_f\right) + \varepsilon\sigma A(T^4 - {T_a}^4) \quad (2.5)$$

Where,

h= heat transfer coefficient, $W/m^2.K$

A= Surface area for heat transfer, $m^2$

T= Cell temperature, K

$T_f$= Cooling Fluid temperature, K

$\varepsilon =$ Emission ratio

$\sigma =$ Steffan-boltzman constant= $5.69*10\text{-}8\ Wm^{-2}K^{-4}$

$T_a$= Ambient Temperature, K

The first term in eq. (2.5) represents the convective heat transfer and the second term is the heat transfer due to radiation.

The description of the energy balance is another approach to explain the cell's heat flow. The difference between the rate of heat generation within the cell and the rate of heat rejection is the heat accumulation which determines the temperature change. [30]

$$mc_p \frac{dT}{dt} = Q_g - Q_d \quad (2.6)$$

Where,

m= mass of the cell, g

cp= effective specific heat capacity of the cell, J/g.K

**C rate:** C rate is the rate at which battery is charged or discharged. [31]

C rate= Current X Battery Capacity.

## 2.6. Battery reference model

As shown in the figure 4, equivalent circuit models of batteries serve as common battery reference models because they accurately represent the current/voltage dynamics of batteries. SOC is the only internal electrochemical state in the circuit model, which is a downside. The resistive/capacitive states of the model are useful in anticipating the approach of battery terminal voltage to voltage limits but offer no physical insight into the workings of the internal processes of the battery. [6]

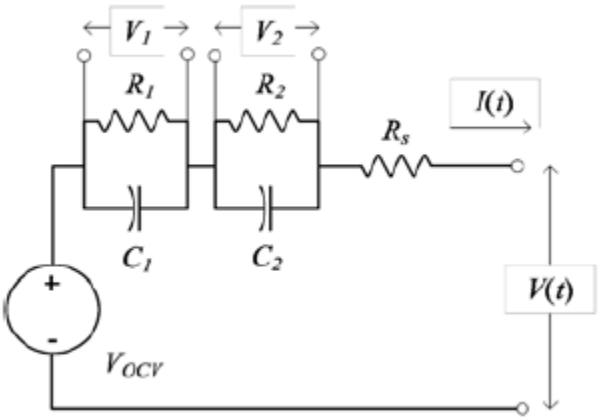


*Figure 4: Continous time state variable model of battery equivalent circuit [6]*

From reference [6],
In this model the state equation be

$$\dot{x}(t) = Mx(t) + NI(t) \qquad (2.7)$$

Where, $u(t) = I(t)\ and\ y(t) = V(t)$

The output equation be

$$V(t) = Ox(t) + PI(t) + y_0 \qquad (2.8)$$

In these equations, x is a vector of model states, y is a vector of the model outputs, and u is a vector of model inputs.

State-of-charge (SOC),

$$SOC(t) = SOC_0 - \int_0^t \frac{I(t)dt}{Q} \qquad (2.9)$$

Where, Q= battery capacity
$SOC_0$= Initial SOC
State vector, x= [SOC;V1;V2]

Eigen values, $\lambda_i = \frac{-1}{R_i C_i}$

State matrix, M=[0 0 0;0 $\lambda_1$ 0;0 0 $\lambda_2$]

Input Matrix, N=[$-\frac{1}{Q}$;$\lambda_1 R_1$;$\lambda_2 R_2$]

Time derivative, $\dot{x}$= $\frac{dx}{dt}$

Output matrix, O= [$\frac{\delta U}{\delta SOC}$ -1 -1]

Feedthrough matrix, P= $[R_s]$

Constant term at the linearization setpoint, $SOC_{setpt}$

$$y_0 = V_{ocv,setpt} - \frac{\delta V_{oc}}{\delta SOC}\Big|_{SOC_{setpt}} * SOC_{setpt} \quad (2.10)$$

The constraint is usually minimum and maximum cell terminal voltage. A general constraint in the model output is-

$$y_{min} < y(t) < y_{max} \quad (2.11)$$

Another constraint is $T_{min}<T<T_{max}$. (2.12)

The limiting current is

$$\boldsymbol{I_{min/max,\Delta t} = [OM^* N + P]^{-1}\{(y_{lim} - y_0) - Oe^{M(\Delta t)}\hat{x}\}} \quad (2.13)$$

# 3. Battery Management System Incorporating Dynamic Power Limiting with Thermal Management

Dynamic power limits in a Battery Management System (BMS) are implemented to ensure the battery operates safely during charging and discharging. To accomplish this, the BMS monitors important battery parameters such as temperature, voltage, current, and state of charge (SOC) to calculate the maximum permissible charging and discharging power. The BMS serves as a management technique for rechargeable batteries, enabling the monitoring and calculation of diverse battery parameters. BMS can be categorized as either simple or complex. A simple BMS regulates voltage levels and restricts current flow when predetermined thresholds are reached. On the other hand, a more sophisticated BMS monitors various battery parameters to optimize battery lifespan and efficiency.

## 3.1. Software Tools

For the analysis and design of systems and products, engineers and scientists can use the programming environment called MATLAB. The MATLAB language, a matrix-based language that enables the most natural expression of computer mathematics, is the core of MATLAB. This tool can do data analysis, mathematical modeling, parallel computing, and algorithm development as well. In this thesis, MATLAB has been employed to simulate and control the different aspects of lithium-ion batteries.

Figure 5 below shows proposed the algorithm for dynamic power limits in BMS. This is explained below step by step.

## 3.2. Selection of Battery Cell Type

In this step, the selection of the appropriate battery cell type is crucial. Different cell geometries such as cylindrical, prismatic, or pouch cells may have varying characteristics and performance [32]. This selection is based on available literature data and considerations specific to the research objectives.

## 3.3. Development of heat transfer model

The development of a heat transfer model is essential to accurately analyze the thermal behavior of the battery. This model considers the heat generation and heat rejection mechanisms. It involves the establishment of mathematical equations or algorithms that describe the heat transfer processes within the battery. Factors such as State of Charge (SOC), and temperature are considered to model the heat transfer phenomena accurately. The heat generation also varies for different cell chemistries. In ref [28], the study presents expressions or values of internal electrical resistance for various cell types, such as LMO, LFP, SONY-US50G3, Sony 18650, and Lithium-Ion Polymer Battery. Furthermore, the heat dissipation from batteries is crucial for maintaining optimal temperature during operation. The model considers heat dissipation through conduction, convection, and radiation. The dependencies of heat generation and dissipation on SOC, and temperature are also considered. Equation (2.3) provides the representation of the internal electrical resistance (Re) in terms of temperature and estimated SOC, allowing for a more accurate estimation of heat

generation based on these factors. Additionally, the model acknowledges the impact of temperature on reversible entropic heat generation and considers temperature variations throughout the battery.

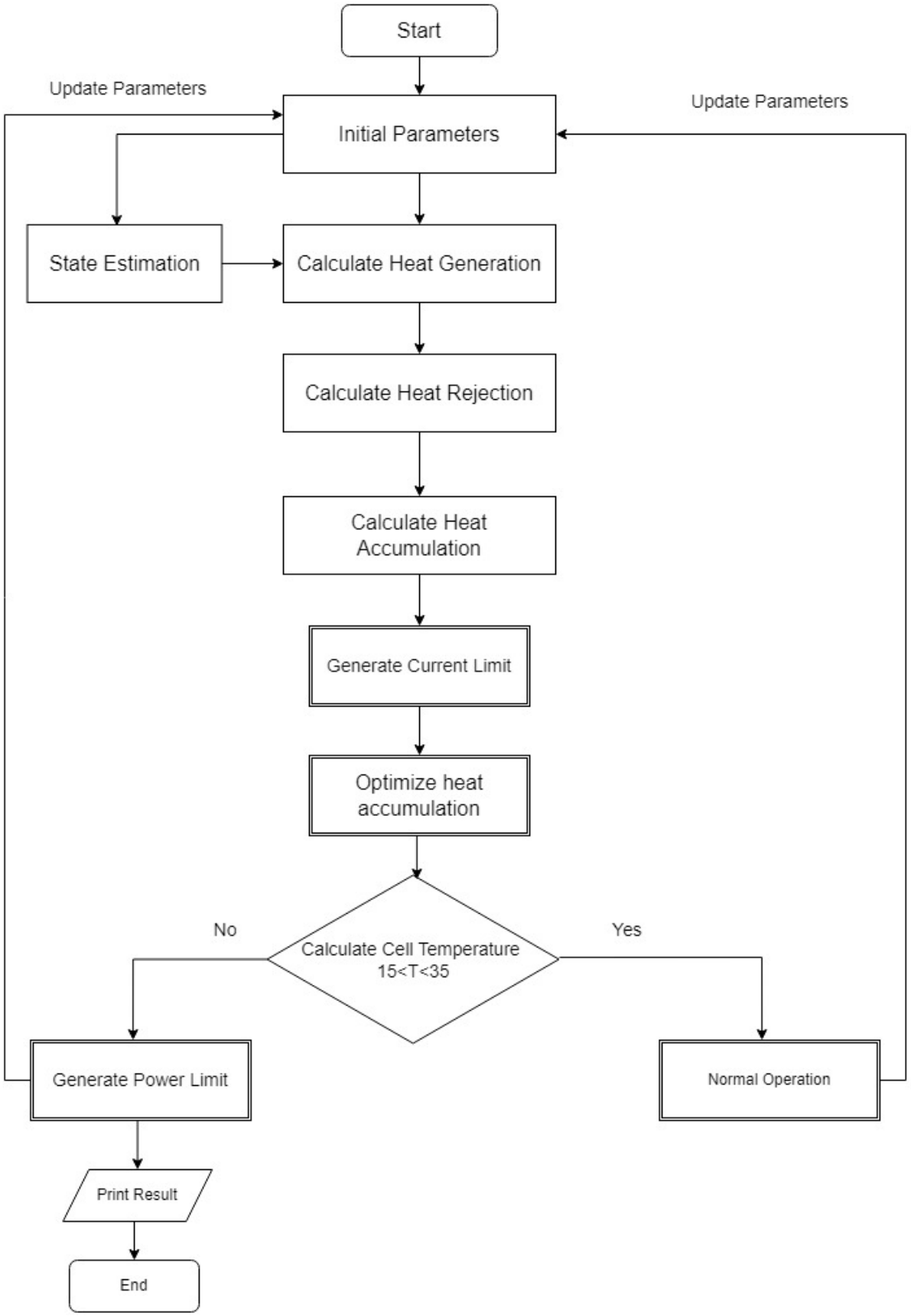


*Figure 5: Proposed algorithm for Power limits in Battery Management System*

## 3.4. Estimation Methods of Battery State

Accurately estimating the state of the battery is a vital aspect of Battery Management Systems (BMS) as it allows for effective monitoring of the battery's internal conditions. Key parameters that need to be identified and tracked include the State of Charge (SOC), and State of Power (SOP) of the battery. These parameters provide crucial information for tasks such as efficient charging, proper thermal management, and overall battery health maintenance. This modeling-based approach is widely utilized in Electric Vehicle (EV) applications to ensure optimal battery performance and longevity.

## 3.5. Optimization/Limit function

To quantify the amount of heat being accumulated in a cell during charge and discharge, a suitable objective function in the context of optimization can be used. The primary objective of this function will be to reduce the heat accumulated in the cell. One approach can be to define a heat accumulation function that considers various factors such as current, resistance, temperature, and time. This function calculates the integral of the power dissipation over the duration of charge or discharge.

To develop an optimization function that calculates a dynamic current limit for the battery, taking into account heat accumulation and temperature constraints, several steps can be followed. First, the continuous and peak current limits of the battery need to be defined. Additionally, the desired temperature limit for the battery is determined which is 15℃ to 35℃. Next, time periods for which the current limit needs to be calculated, such as 1 min, 5 min, and 30 min, must be set. In addition, maximum and minimum SOC limits also need to be considered. An optimization algorithm can then be developed to consider the heat generated during the charge and discharge processes. The C rates, which indicate the rate of charge or discharge, should be taken into consideration as they influence heat generation. The internal energy function, calculated by multiplying the current, resistance, and time, can be used to quantify the heat accumulated in the cell. With this information, the optimization function can be designed to dynamically adjust the current and power limits for future time periods based on the heat accumulation from previous periods. It is crucial to ensure that the battery temperature remains within the prescribed limit by adjusting the current limit accordingly. The developed optimization function should be validated through simulations and experimental testing to ensure its effectiveness. By implementing this dynamic optimization function, it becomes possible to control the current limits of the battery, preventing excessive heat generation and maintaining the battery's temperature within safe operating conditions.

$$E = \sum_{t=0}^{N} I^2 * R * t \qquad (3.1)$$

Where, E is the internal energy
I is the current
R is the resistance
t is the time.
N is the number of intervals

To ensure that the internal energy function remains within acceptable limits, it is important to define upper and lower bounds for the function. The upper bound represents the maximum internal energy that the battery can safely handle without risking overheating or degradation, while the lower bound represents the minimum internal energy required for efficient operation. By setting these bounds, the heat accumulation within the battery can be effectively managed. To determine appropriate current limits based on usage for different time periods, an analysis considering the heat generation and heat dissipation characteristics of the battery is essential. This analysis can involve developing mathematical models or employing simulation techniques to predict the internal energy accumulation and the corresponding temperature changes over time. By carefully considering the heat generation and heat transfer mechanisms, and incorporating the limits on the internal energy function, it is possible to derive optimal current limits that ensure safe battery operation while maximizing its performance and longevity.

# 4. Results and Discussion

The outcomes of the Battery Management System (BMS) combining Dynamic Power Limiting and Thermal Management Systems are covered in this chapter. In this thesis, a standard LFP cylindrical cell has been taken into account.

## 4.1. Irreversible heat in the battery cell

The production of irreversible heat within the battery cell as a function of both temperature and state of charge (SOC), is shown in figure 6. When the temperature increases the generation of irreversible heat is more. On the other hand, at lower SOCs, more irreversible heat is produced inside the battery.

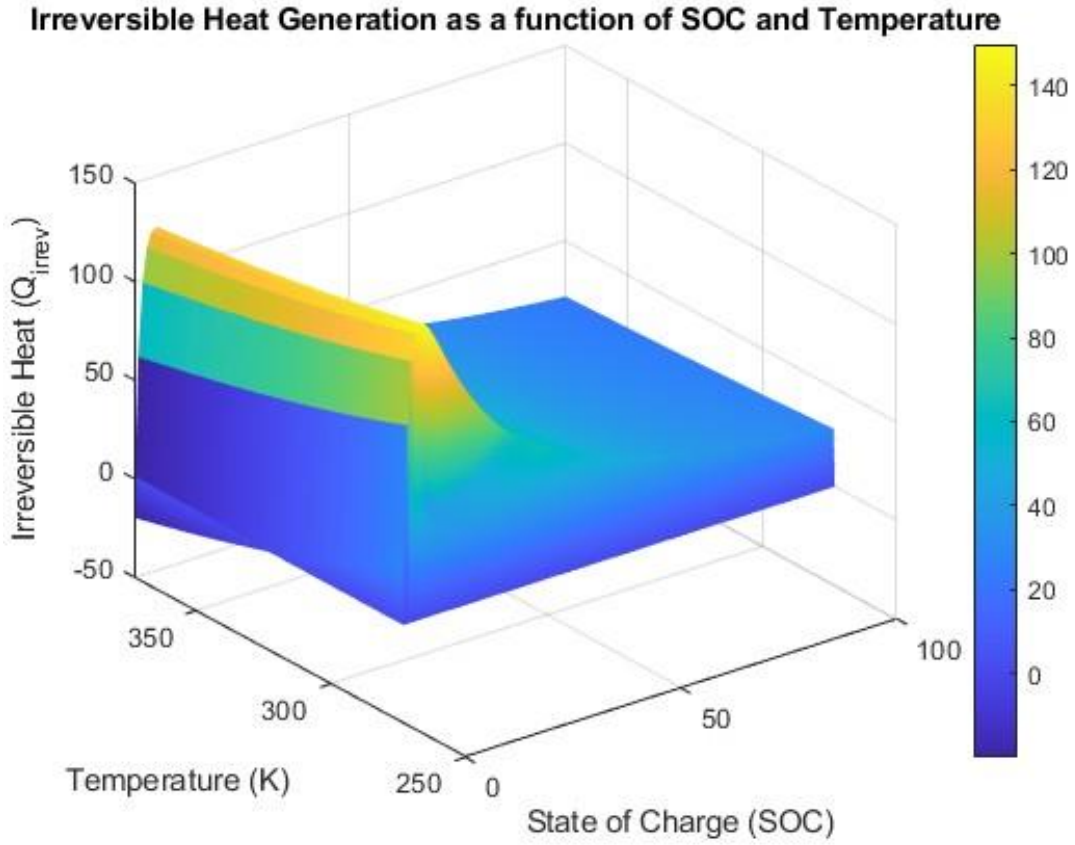


*Figure 6: Irreversible heat as a function of SOC and temperature*

From figure 6, understanding how SOC and temperature interact is crucial for comprehending the battery's heat generating characteristics. As seen in the figure, a rise in temperature causes the battery's internal heat production to rise in direct proportion. Higher temperatures speed up internal resistive losses and chemical reactions, increasing the rate of heat generation. Because thermal impacts are more obvious under high-temperature operating settings, this phenomenon is particularly important. It emphasizes the significance of efficient thermal management techniques to reduce excessive heat generation and keep batteries operating at their best. The image, on the other hand, shows how low SOC levels cause a greater production of irreversible heat inside the battery cell. The battery experiences deeper discharge cycles when the SOC is low, which could result in a higher internal resistance and greater resistive losses. These losses cause the battery to generate

heat that cannot be reversed, which exacerbates the heat production overall. For efficient power limit algorithms and thermal management solutions, it is essential to comprehend how SOC and temperature affect irreversible heat generation. This knowledge can be incorporated into the algorithm's design to enable dynamic power limit adjustments based on SOC and temperature data in real-time. This adaptive strategy aids in avoiding excessive heat accumulation, protecting battery health, and improving system performance. Figure 6 shows the relationship between temperature, SOC, and irreversible heat generation. The graph shows that while low SOC levels are to blame for more irreversible heat generation, higher temperatures contribute to increasing heat production within the battery. This knowledge makes it possible to create dynamic power limits algorithms that take these elements into account, improving both thermal management and battery performance.

## 4.2. Reversible heat in the battery cell

Regarding SOC and current polarity, the findings shown in Figure 7 and 8 offer insightful knowledge into the reversible heat generation within a Li-ion battery cell.

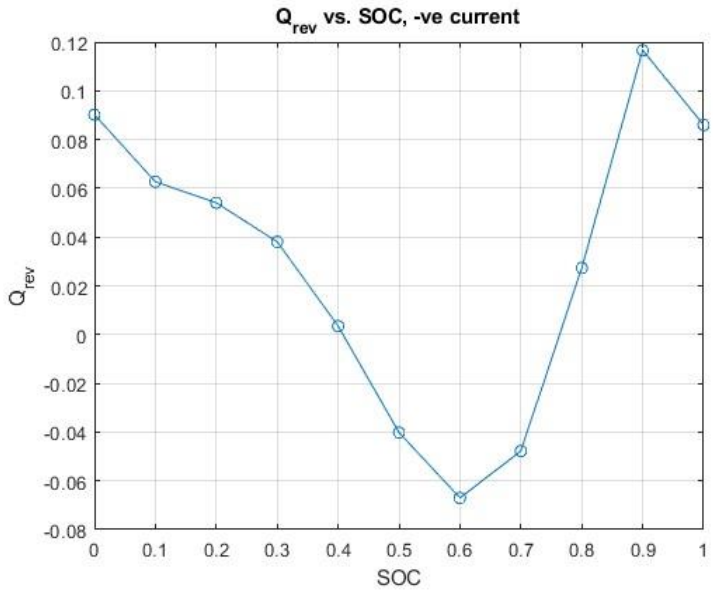


*Figure 7: Reversible heat as a function of SOC, for charging*

Figure 7 shows the relationship between SOC and the reversible heat generation in the Li-ion battery cell. The results show that the reversible heat generation ($Q_{rev}$) has a positive value for SOC values between 0 and 0.4 and 0.75 and 1.0. This shows that the heat produced inside the battery cell during certain SOC ranges is reversible and can be recovered or used. On the other hand, the reversible heat generation turns negative for SOC levels outside of these ranges. This indicates that there is a permanent waste of energy because the heat produced during these SOC intervals is not easily retrieved or recycled. The fact that a negative current is present during these times is significant since it shows that the battery is charging. Figure 8 shows under conditions of positive current, the reversible heat generation within the Li-ion battery cell is examined in this figure. It is interesting to note that the phenomenon in this instance is the opposite of that in Figure 7.

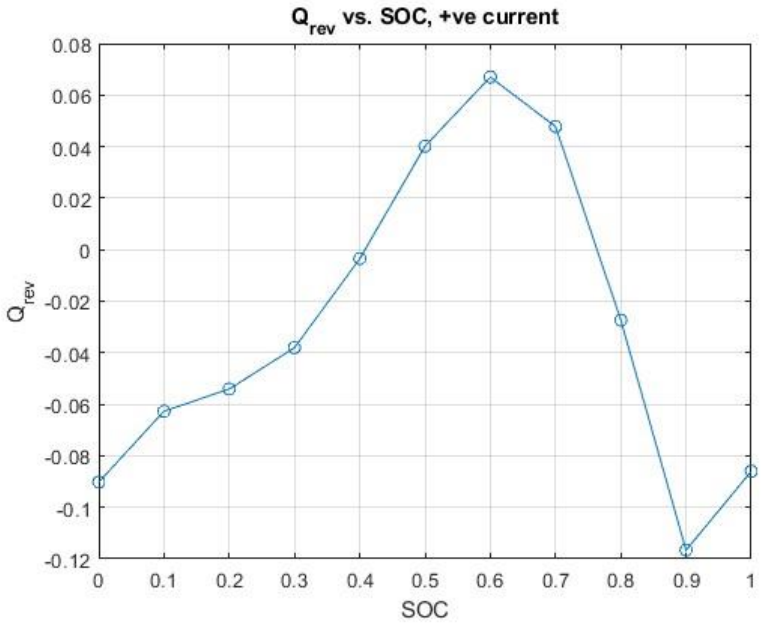


*Figure 8: Reversible heat as a function of SOC, for discharging*

For SOC values between 0.4 and 0.75, positive heat generation is seen, whereas for all other SOC values, negative heat generation is seen. When the current is positive, the battery cell is charging if the positive heat generation is within the SOC range of 0.4 to 0.75. The battery is storing energy while charging, which causes reversible heat generation that can be captured or used. Overall, these findings offer a thorough understanding of the heat generating phenomena—both reversible and irreversible—within Li-ion battery cells. Researchers and engineers can create effective thermal control mechanisms, optimize battery management tactics, and improve overall battery performance and lifespan by considering the relationship between SOC, current polarity, and heat generation. The heat produced during the charging process is not easily recovered or reusable, which represents an irreversible loss of energy.

## 4.3. Total Heat Generation inside the cell

The results that are shown shed light on how a battery generates heat at various rates and lengths of charging and draining. Figure 9 shows that the battery generates about 80 J of heat when it is charged and drained at rates between 0.1C and 0.2C over a period of one minute. The higher current flow brought on by the faster charging and discharging rates has an impact on this heat generation.

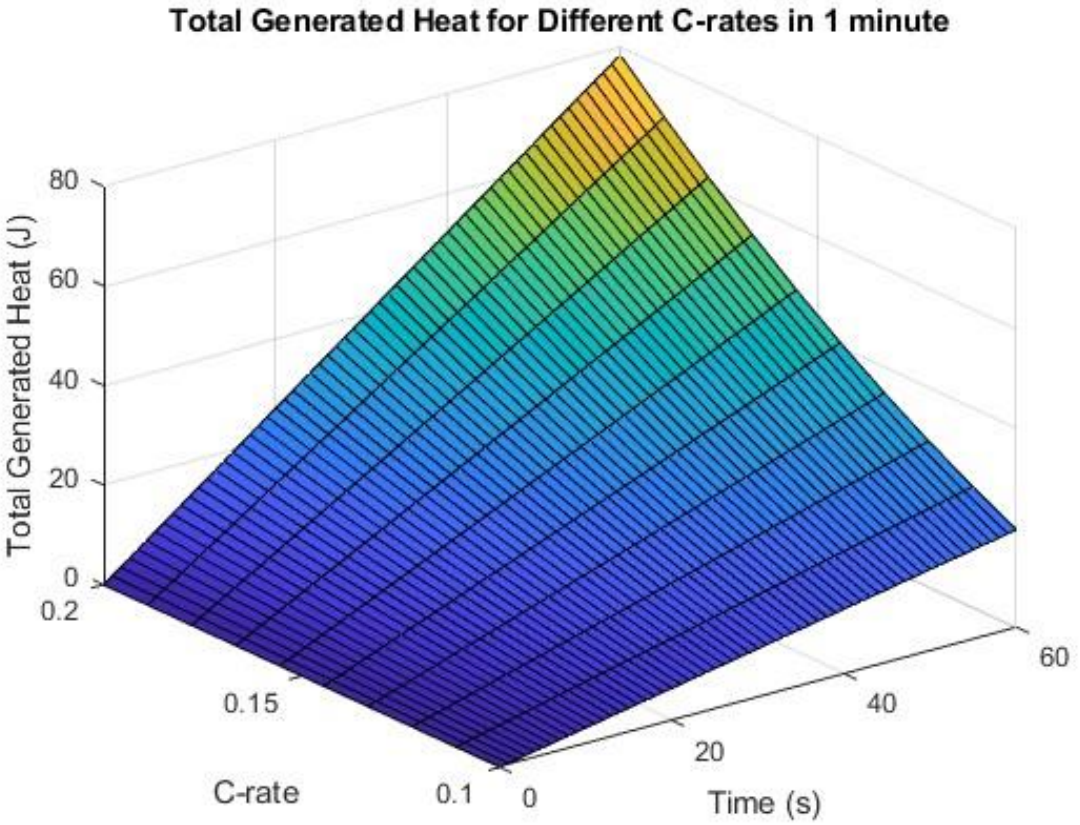


*Figure 9: Total Heat generation inside the cell for charge and discharge at different C rates for 1 minute*

Figure 10 elaborates on these findings by showing that the heat generation increases noticeably to roughly 400 J when the battery is charged and drained at the same rates of 0.1C to 0.2C but for a longer period of time of five minutes. The prolonged operation duration, which permits a greater quantity of energy transfer within the battery and increases heat generation, is to blame for this significant increase in heat output.

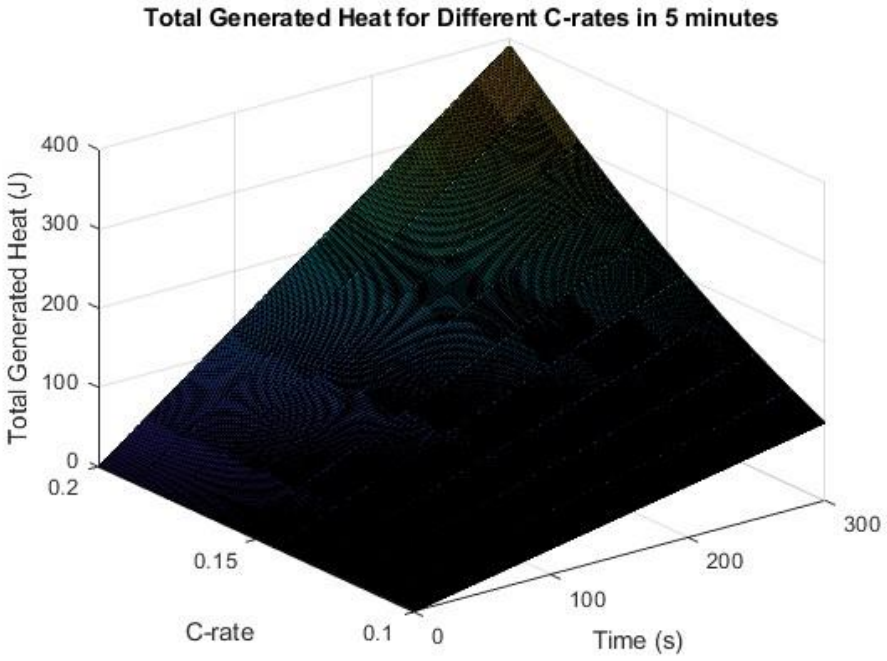


*Figure 10: Total heat generation inside the cell for charge and discharge at different C rates for 5 minutes*

Figure 11 also shows the heat produced when the battery is charged and drained for a prolonged duration of 30 minutes at rates between 0.1C and 0.2C. In this instance, the heat produced is around 2400 J, demonstrating a significant increase over the shorter times. A greater amount of energy may be transferred within the battery due to the longer operating time, which increases heat generation.

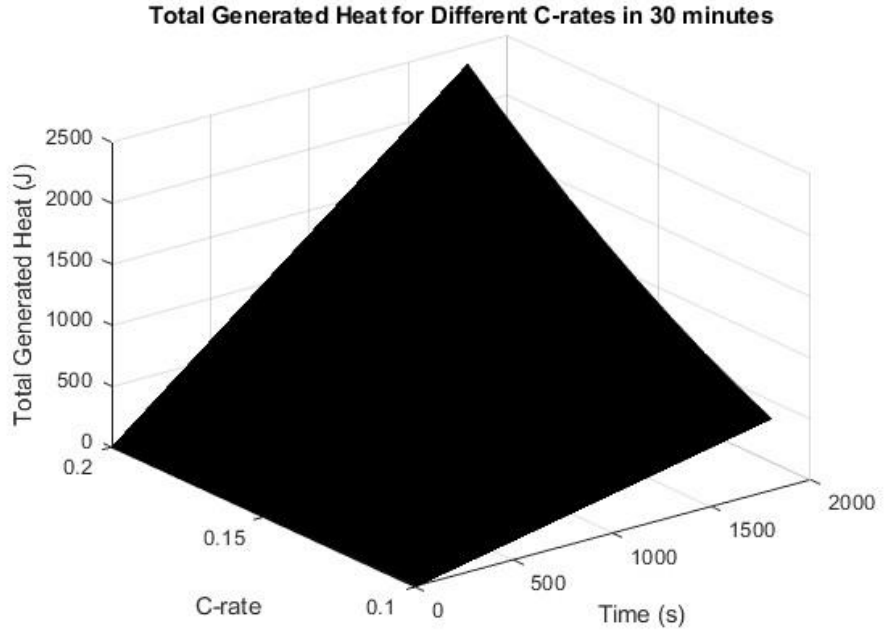


*Figure 11: Total Heat generation inside the cell for charge and discharge at different C rates for 30 minutes*

These findings highlight the impact of time and charging/discharging rates on battery heat generation. More energy is transported within the battery as the rates and durations rise, which corresponds to an increase in heat output. Understanding and controlling the thermal behavior of

batteries, especially in applications with higher current requirements or longer operating times, depends heavily on this information.

It is possible to create efficient thermal management methods for the battery system by quantifying the heat generation under various charging and discharging scenarios. These tactics can entail using the proper cooling techniques or creating battery packs with improved heat dissipation capacities. Furthermore, these discoveries have applications for battery usage and design. They emphasize the importance of carefully weighing the proper charging and discharging rates and durations considering the requirements of the individual applications. By maximizing energy efficiency while minimizing heat output, it is feasible to improve the battery system's overall performance and dependability.

## 4.4. Accumulated heat inside the battery cell

A portion of the heat produced by the battery cell is dissipated into the environment when it is subjected to cooling methods such air or liquid cooling, while the remaining heat is accumulated inside the cell. An investigation of the battery cell's internal heat accumulation phenomenon is provided in this section. The results shown in Figures 12, 13, and 14 offer insightful information about the development of heat within the battery cell under various charging and discharging situations.

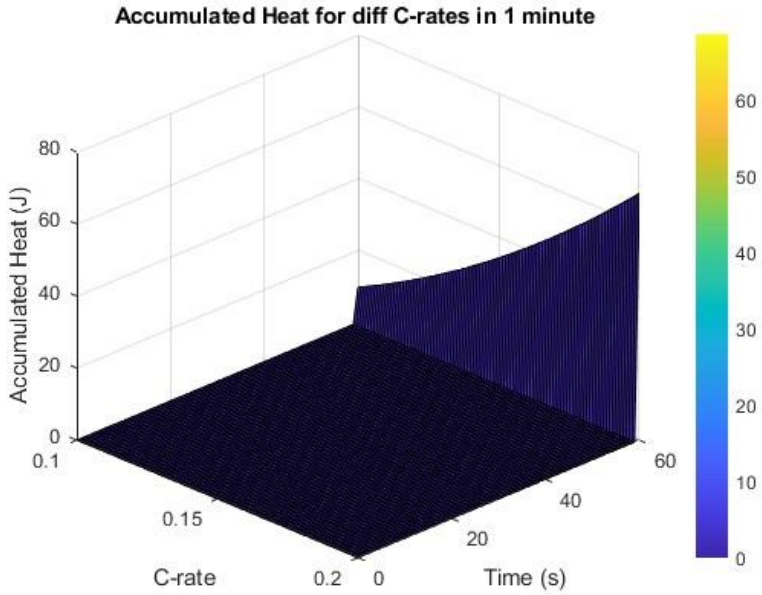


*Figure 12: Accumulated heat inside the cell for charge and discharge at different C rates for 1 minute*

Figure 12 shows that the accumulated heat inside the cell reaches an estimated value of 70 J when the battery is subjected to charge and discharge procedures at C rates ranging from 0.1C to 0.2C for a duration of one minute. The rate of energy transfer, the chemistry of the batteries, and how well the cooling system is working all have an impact on the heat buildup. Understanding and controlling heat accumulation is essential because too much heat can negatively impact battery performance and lifespan.

Adding more detail, Figure 13 shows that the accumulated heat inside the cell dramatically rises to about 350 J when the battery is subjected to charge and discharge cycles at the same C rates but for a longer time of five minutes. As a result of the increased energy transfer possible due to the longer operation time, the battery can store more heat. These results emphasize the value of taking into account the length of charge and discharge cycles when analyzing heat accumulation and applying suitable thermal management techniques.

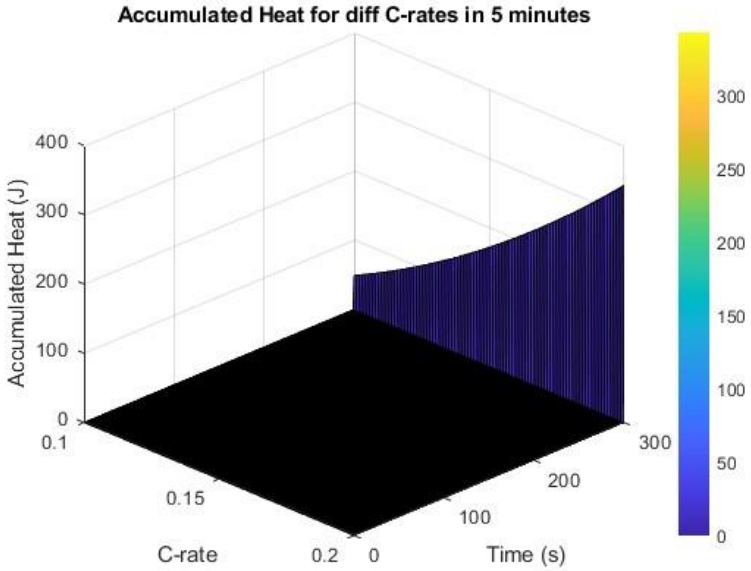


*Figure 13: Accumulated heat inside the cell for charge and discharge at different C rates for 5 minutes*

Figure 14 shows how heat builds up inside the battery cell over an even longer period of time, 30 minutes. It reveals that the accumulated heat inside the cell reaches about 1750 J when the battery is charged and drained at varied C rates ranging from 0.1C to 0.2C for this prolonged period. This significant increase in heat accumulation compared to shorter times underlines the importance of adequate cooling methods and efficient heat dispersion in order to prevent an excessive temperature rise.

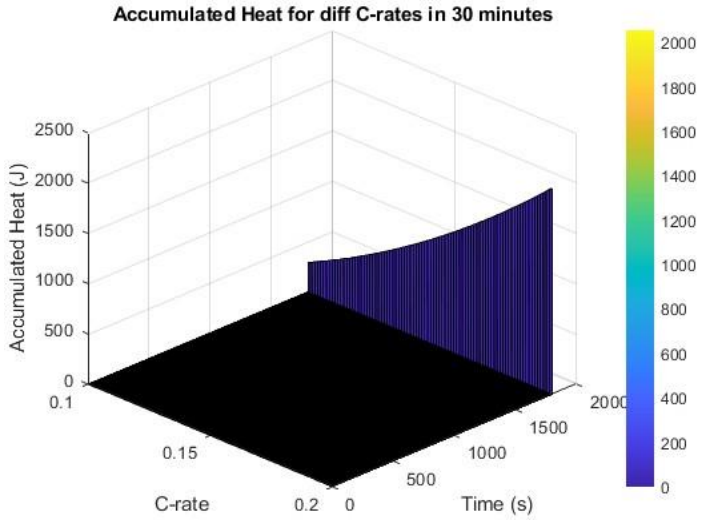


*Figure 14: Accumulated heat inside the cell for charge and discharge at different C rates for 30 minutes*

To summarize, the results shown in Figures 12, 13, and 14 provide insight into the heat buildup process that occurs under various charging and discharging conditions. They emphasize the significance of putting into practice efficient thermal management techniques to reduce heat buildup and keep the battery at safe operating temperatures. It is feasible to minimize heat-related problems and guarantee the reliable and effective operation of battery systems by carefully monitoring charge and discharge durations and taking appropriate cooling solutions into consideration.

## 4.5. Optimized heat

The primary objective of optimization is to optimize the heat that has been accumulated in the cell. To achieve this, the current has been limited to minimize the heat. To limit the current, the C rate has been reduced. The outcomes shown in Figures 15, 16, and 17 show how well the optimization function for controlling heat generation in batteries during charging and discharging procedures that was developed in the thesis performs. The optimal heat values for various C rates and durations are shown in the figures.

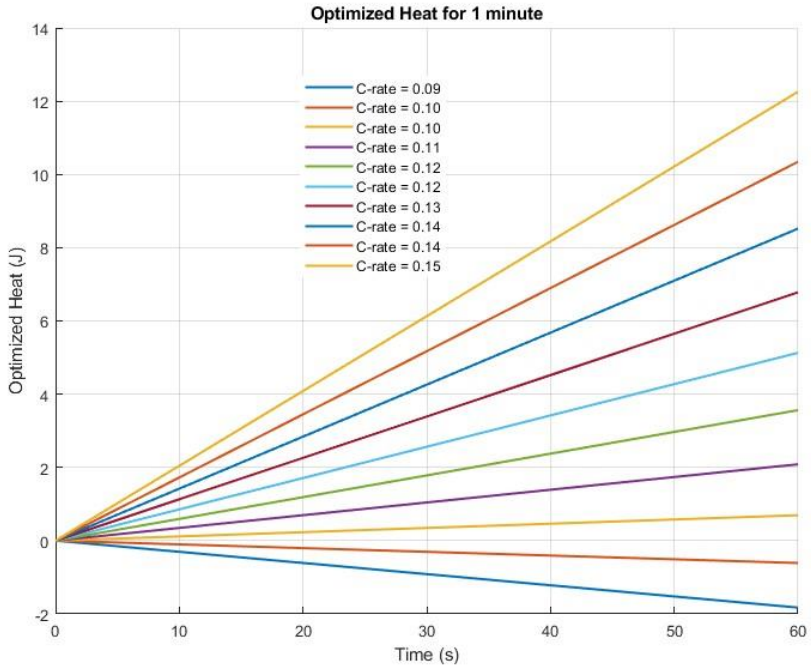


*Figure 15: Optimized heat inside the cell for charge and discharge at various C rates for 1 minute*

Figure 15 focuses on a charging and discharging cycle lasting one minute. For C rates between 0.09C and 0.15C, the optimal heat values fall between -2J and +12J. This shows that the optimization function can efficiently control heat generation in a short amount of time.

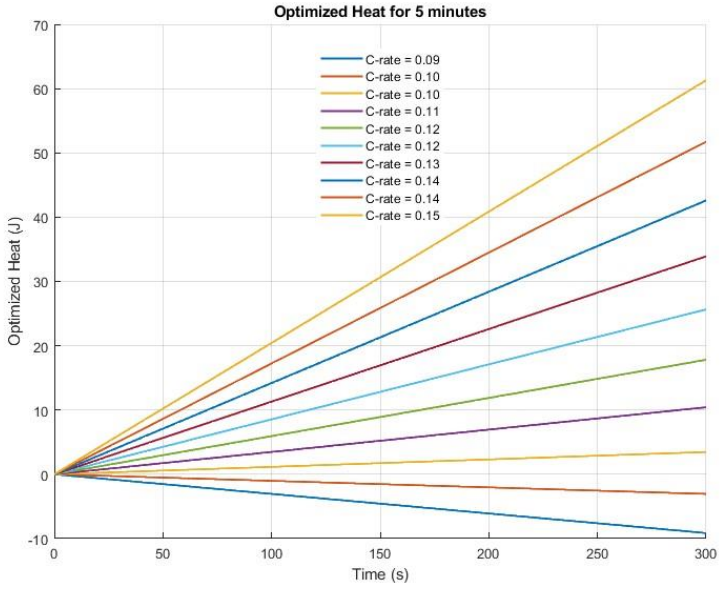


*Figure 16: Optimized heat inside the cell for charge and discharge at various C rates for 5 minutes*

The results for a 5-minute charging and discharging period are shown in Figure 16. For C rates between 0.09C and 0.15C, the optimum heat values in this instance range from -10 J to roughly 60 J. This demonstrates that although the optimization algorithm continues to work effectively as the length rises, the heat generation range does as well.

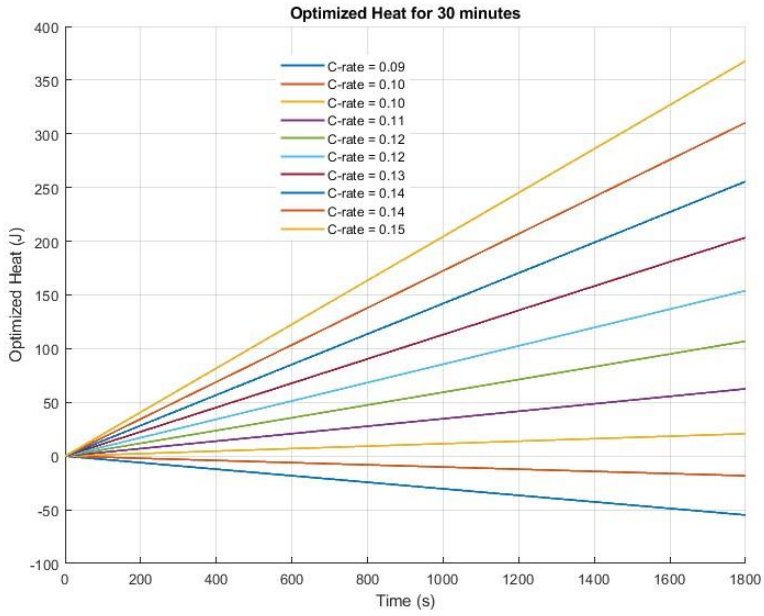


*Figure 17: Optimized heat inside the cell for charge and discharge at various C rates for 30 minutes*

Figure 17 looks at a longer charging and discharging time of 30 minutes. The optimal heat values are for C rates between 0.09C and 0.15C, and they range from -60 J to roughly 370 J. According to this finding, the optimization function manages heat generation as the time lengthens, but the range of heat values widens even more.

It is evident that these heat levels are significantly lower than what would be produced in the absence of the current limiting and optimization procedure, although being higher than the preceding scenario. The optimization strategy successfully controls and reduces the buildup of heat inside the battery cell by further lowering the C rate. These findings demonstrate how well the optimization strategy works at reducing heat collection and generation inside battery cells by managing current flow. This procedure successfully limits the energy transfer and electrochemical reactions, resulting in less heat generation. This is done by lowering the C rate. The obtained optimal heat values show that the method can successfully control and reduce heat accumulation in various operational conditions. For the battery to be thermally stable, safe, and long lasting, heat accumulation must be optimized. The risk of thermal runaway, deterioration, and other negative impacts can be reduced by reducing excessive heat generation. Furthermore, by lowering energy losses and enhancing thermal management measures, the optimization approach enhances the battery system's overall performance and efficiency.

In conclusion, the thesis's optimization function shows that it can control heat production in batteries during charging and discharging processes for a range of C rates and durations. To maintain effective heat management for longer periods of time, the optimization function may encounter difficulties when the range of optimized heat values expands with duration.

## 4.6. Power Limits as a function of limiting current and temperature

Since the heat accumulation in the battery cell has been optimized now, the battery reference model, which has already been presented in chapter 2, can be utilized to find the power limit of the battery to operate it within the optimal temperature range of 15 ℃ to 35 ℃ to ensure the maximum output from the battery and maintaining safety as well. Figures 18 and 19 below show the results after the power limit has been employed. Here power limits are demonstrated as a function of limiting current and temperature.

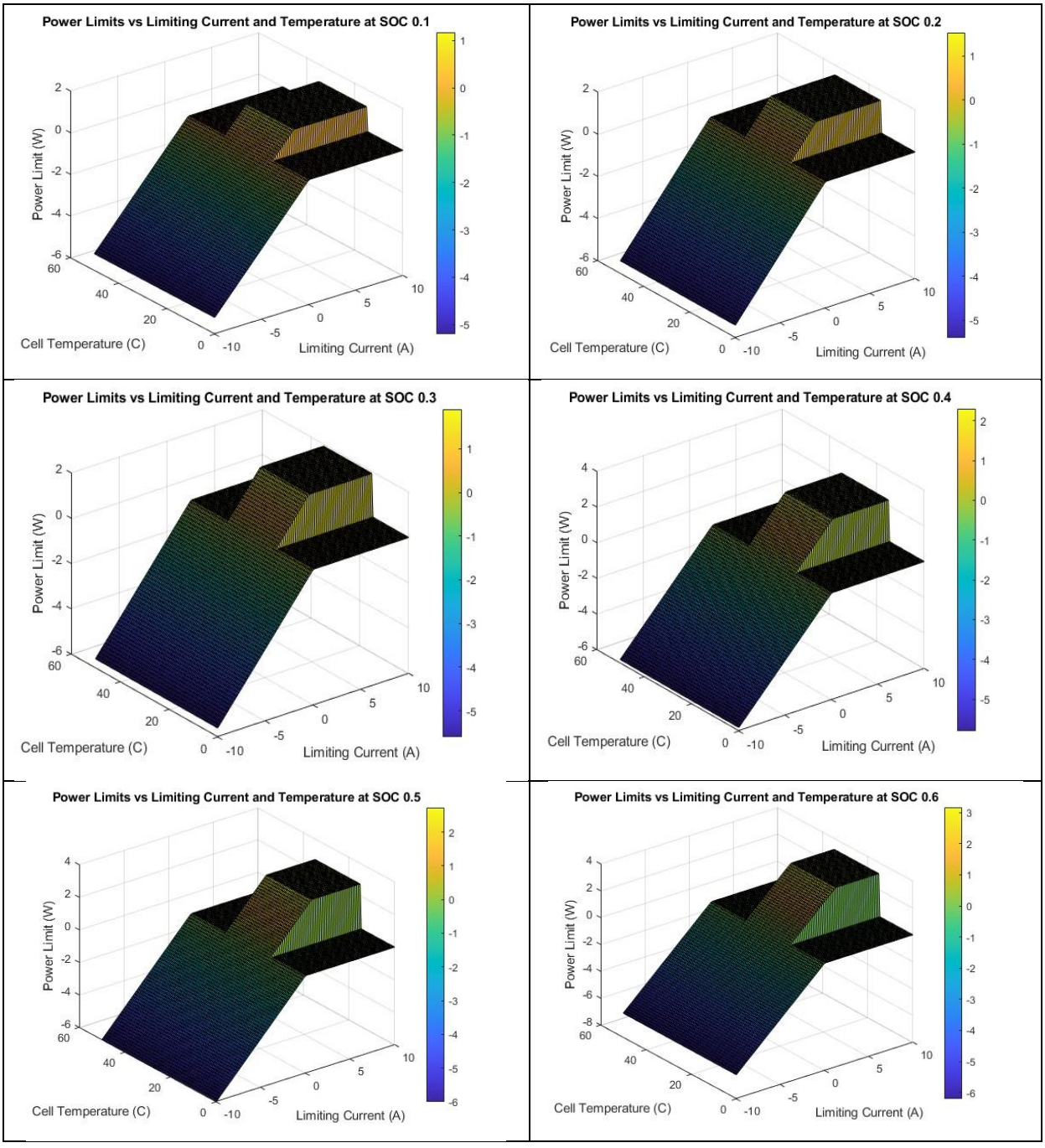


*Figure 18: Power limit as a function of current limit and cell temperature at SOC 0.1 to 0.6*

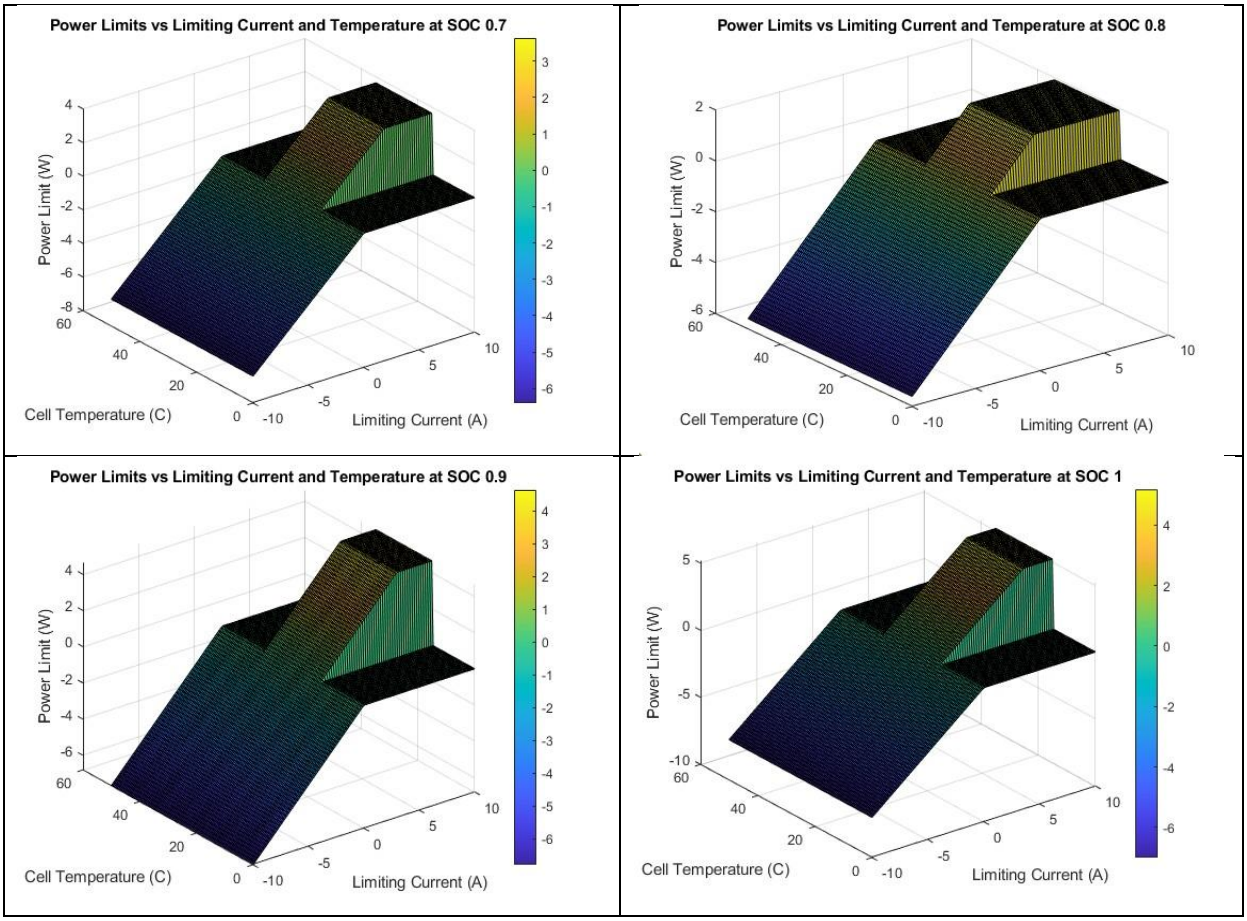


*Figure 19: Power limit as a function of current limit and cell temperature at SOC 0.7 to 1.0*

As the figures 18 and 19 illustrate, the maximum power output from the battery is dependent on the SOC level. From the figures, it is evident that higher SOC levels offer higher output from the battery and vice versa.

Additionally, the results, as in the figures 18 and 19, show significant influence of temperature on power limits. As the temperature increases, the power limits of the battery system will be decreased. This can be attributed to the increased heat generation within the battery cells and the reduced heat dissipation efficiency at higher temperatures. The relationship between temperature and power limits follows a nonlinear trend. At optimum temperatures, the power limits will be relatively higher, indicating improved performance and power transfer capabilities of the battery. However, as the temperature exceeds certain thresholds, the power limits will start to decrease rapidly, imposing constraints on the power output of the battery system. The findings highlight the importance of temperature management in maintaining optimal power limits. Effective thermal management techniques, such as active cooling systems or temperature regulation algorithms, are essential to ensure that the battery operates within its optimal temperature range and maximizes its power output.

Furthermore, the analysis demonstrates that SOC and temperature fluctuations can impact the stability and reliability of power limits. Rapid temperature changes or temperature cycling can lead to dynamic variations in the power limits, affecting the overall performance and efficiency of the battery system. To mitigate the effects of temperature on power limits, it is crucial to incorporate

temperature monitoring and control mechanisms into the BMS. By continuously monitoring the temperature and adjusting the power limits based on the thermal conditions, the BMS can optimize the power management strategy and maintain safe and efficient battery operation. In summary, the effect of temperature on power limits underscores the importance of temperature regulation and thermal management in the BMS. By carefully controlling the temperature within the desired range, the BMS can ensure optimal power output, prolong the battery life, and enhance the overall performance and reliability of the battery system.

## 5. Conclusion

This thesis aimed to develop a dynamic algorithm for updating power limits in a BMS based on battery usage. Here is a summary of the major points considering the research questions:

- The model produced an accurate estimate of the heat produced by the battery cell by considering factors including battery chemistry, temperature, and SOC.
- The effect of temperature and SOC on heat production have been examined and documented. These results underlined how important it is to control temperature and SOC levels to maximize power limits and minimize heat-related problems.
- The simulation outcomes showed how well the created model performed in calculating heat accumulation during charging and discharging process throughout a variety of time periods.
- In order to efficiently control heat accumulation and prevent an excessive temperature rise inside the battery cell, a specialized function has been proposed. The performance, longevity, and safety of the battery are all enhanced by this feature.
- The battery reference model was utilized to produce desired outcome with all the constraints.
- Through extensive modeling and simulation work in MATLAB, the algorithm's effectiveness was evaluated, and the results were analyzed.
- The algorithm was successful in determining limits on power that successfully controlled the heat generated and accumulated inside the battery cell by taking into account the intended time periods. By setting these power limits, the battery will be able to operate safely and effectively while avoiding overheating and hazardous thermal runaway.

Due to time constraints, it was not possible to integrate the developed algorithm into the existing BMS for battery applications like EV, PV etc. This process is a difficult undertaking that calls for careful consideration of hardware and software interfaces, communication protocols, and system-specific needs to integrate a new algorithm into an existing BMS. In order to guarantee seamless integration and dependable performance under real-world operating circumstances, it entails thorough testing, validation, and optimization. Despite the fact that the integration process could not be finished within the study's time frame, the algorithm's design and development were motivated by the desire to aid future integration efforts.

## 6. Future Works

The developed algorithm in this thesis can be integrated into the existing BMS for battery applications like EV, PV etc.

## 7. List of References


[1] Yikai Jia, Sha Yin, Binghe Liu, Hui Zhao, Huili Yu, Jie Li and Jun Xu, "Unlocking the coupling mechanical-electrochemical behavior of lithium-ion battery upon dynamic mechanical loading," *Energy,* vol. 166, p. 951_960, 2019.

[2] Xiao-Hu Yang, Si-Cong Tan and Jing Liu, "Thermal management of Li-ion battery with liquid metal," *Energy Conversion and Management,* vol. 117, pp. 577-585, 2016.

[3] Yoshiyasu Saito, Katsuhiko Kanari and Kiyonami Takano, "Thermal studies of a lithium-ion battery," *Journal of Power Sources,* vol. 68, pp. 451-454, 1997.

[4] Evans, Yufei Chen and James W., "Heat Transfer Phenomena in Lithium/Polymer-Electrolyte Batteries for Electric Vehicle Application," *J. Electrochem. Soc.,* vol. 140, p. 1833, 1993.

[5] Fangdan Zheng, Jiuchun Jiang, Bingxiang Sun, Weige Zhang and Michael Pecht, "Temperature dependent power capability estimation of lithium-ion batteries for hybrid electric vehicles," *Energy,* vol. 113, pp. 64-75, 2016.

[6] Shriram Santhanagopalan, Kandler Smith, Jeremy Neubauer, Gi-Heon Kim, Matthew Keyser, Ahmad Pesaran, Design and Analysis of Large Lithium-Ion Battery Systems, Artech house, 2015.

[7] Bragadeshwaran Ashok , Chidambaram Kannan, Byron Mason, ORCID, Sathiaseelan Denis Ashok, Vairavasundaram Indragandhi, Darsh Patel, Atharva Sanjay Wagh, Arnav Jain andChellapan Kavitha, "Towards Safer and Smarter Design for Lithium-Ion-Battery-Powered Electric Vehicles: A Comprehensive Review on Control Strategy Architecture of Battery Management System," *Energies,* vol. 15, no. 12, p. 4227, 2022.

[8] Gregeory L. Plett., "High-performance battery-pack power estimation using a dynamic cell model," *IEEE Transactions on Vehicular Technology,* vol. 53, no. 5, pp. 1586 - 1593, 2004.

[9] Alexander Farmann and Dirk Uwe Sauer, "A comprehensive review of on-board State-of-Available-Power prediction techniques for lithium-ion batteries in electric vehicles," *Journal of Power Sources,* vol. 329, pp. 123-137, 2016.

[10] Wladislaw Waag, Christian Fleischer and Dirk Uwe Sauer, "Critical review of the methods for monitoring of lithium-ion batteries in electric and hybrid vehicles," *Journal of Power Sources,* vol. 258, pp. 321-339, 2014.

[11] "Comparative study of reduced order equivalent circuit models for on-board state-of-available-power prediction of lithium-ion batteries in electric vehicles," *Applied Energy,* vol. 225, pp. 1102-1122, 2018.

[12] Shun Xiang, Guangdi Hu, Ruisen Huang,Feng Guo and Pengkai Zhou, "Lithium-Ion Battery Online Rapid State-of-Power Estimation under Multiple Constraints," *Energies,* vol. 11, no. 2, p. 283, 2018.

[13] Tian Ruiyuan, Park Sang-Hoon, King Paul J., Cunningham Graeme, Coelho João, Nicolosi Valeria and Coleman Jonathan N, "Quantifying the factors limiting rate performance in battery electrodes," *Nature Communications,* vol. 10, no. 1, p. Article

number 1933, 2019.

[14] Fengchun Sun, Rui Xiong, Hongwen He, Weiqing Li and Johan Eric Emmanuel Aussems, "Model-based dynamic multi-parameter method for peak power estimation of lithium–ion batteries," *Applied Energy,* vol. 96, pp. 378-386, 2012.

[15] Youngki Kim, Shankar Mohan, Jason B. Siegel and Anna G. Stefanopoulou, "Maximum Power Estimation of Lithium-Ion Batteries Accounting for Thermal and Electrical Constraints," in *ASME 2013 Dynamic Systems and Control Conference*, California, USA, 2013.

[16] J. Shepard, "Battery Power Tips," 14 March 2022. [Online]. Available: https://www.batterypowertips.com/li-ion-batteries-part-1-building-massless-batteries-faq/. [Accessed 16 April 2023].

[17] F. W. J. T. L. G. Y. Naoki Nitta, "Li-ion battery materials: present and future," *Materials Today,* vol. 18, no. 5, pp. 252-264, June, 2015.

[18] J. Zhang, M. Terrones, C. Park, R. Mukherjee, M. Monthioux, N. Koratkar, Y. Kim, R. Hurt, E. Frackowiak, T. Enoki and e. al., "Carbon science in 2016: Status, challenges and perspectives," *Carbon,* vol. 98, pp. 708-732, 2016.

[19] W. Li, B. Song and A. Manthiram, "High-voltage positive electrode materials for lithium-ion batteries.," *Chemical Society Reviews,* vol. 46, pp. 3006-3059, 2017.

[20] T. Placke, R. Kloepsch, S. Dühnen and M. Winter, "Lithium ion, lithium metal, and alternative rechargeable battery technologies," *J. Solid State Electrochem,* vol. 21, p. 1939–1964, 2017.

[21] F. Zheng, M. Kotobuki, S. Song, M. Lai and L. Lu, "Review on solid electrolytes for all-solid-state lithium-ion batteries.," *J. Power Sources,* vol. 389, p. 198–213, 2018.

[22] "Review of Comparative battery energy storage systems (Bess) for energy storage applications in tropical environments," in *IEEE 3rd International Conference on Electro-Technology for National Development (NIGERCON)*, Owerri (Futo), Nigeria, 2017.

[23] Ahmed Pesaran and Shriram Santhagopalan, "Addressing the Impact of Temperature Extremes on Large Format Li-Ion Batteries for Vehicle Applications," in *30TH INTERNATIONAL BATTERY SEMINAR*, Ft. Lauderdale, Florida, 2013.

[24] Todd M. Bandhauer, Srinivas Garimella and Thomas F. Fuller, "A Critical Review of Thermal Issues in Lithium-Ion Batteries," *Journal of The Electrochemical Society,* vol. 158 (3), pp. R1-R25, 2011.

[25] D. Bernardi, E. Pawlikowski and J. Newman, "A general energy balance for battery systems," *J. Electrochem. Soc.,* vol. 132, p. 5, 1985.

[26] Weixiong Wu, Wei Wu and Shuangfeng Wang, "Thermal management optimization of a prismatic battery with shape-stabilized phase change material," *International Journal of Heat and Mass Transfer,* vol. 121, p. 967–977, 2018.

[27] Rajath Kantharaj and Amy M. Marconnet, "Heat Generation and Thermal Transport in Lithium-Ion Batteries: A Scale-Bridging Perspective," *Nanoscale and Microscale Thermophysical Engineering,* vol. 23, p. 128–156, 2019.

[28] Rajib Mahamud and Chanwoo Park, "Theory and Practices of Li-Ion Battery Thermal Management for Electric and Hybrid Electric Vehicles," *Energies,* vol. 15, p. 3930, 2022.

[29] Huaqiang Liu, Zhongbao Wei, Weidong He and Jiyun Zhao, "Thermal issues about

Li-ion batteries and recent progress in battery thermal management systems: A review," *Energy Conversion and Management,* vol. 150, pp. 304-330, 2017.

[30] Elke Schuster, Carlos Ziebert, Andreas Melcher, Magnus Rohde, Hans Jürgen Seifert, "Thermal behavior and electrochemical heat generation in a commercial 40 Ah lithium ion pouch cell," *Journal of Power Sources,* vol. 286, pp. 580-589, 2015.

[31] M. A.-Z. C. D. S. D. A. R. C. H. A. Daniela Galatroa, "THERMAL BEHAVIOR OF LITHIUM-ION BATTERIES: AGING, HEAT GENERATION, THERMAL MANAGEMENT AND FAILURE," *Frontiers in Heat and Mass Transfer,* 2020.

[32] Pengyu Wei, Muhammad Abid,Humphrey Adun,Desire Kemena Awoh,Dongsheng Cai ,Juliana Hj Zaini and Olusola Bamisile, "Progress in Energy Storage Technologies and Methods for Renewable Energy Systems Application," *Applied Sciences,* vol. 13, no. 9, p. 5626, 2023.

[33] S. K. G.-H. K. M. P. A. A. S. Santhanagopalan, Design and analysis of large lithium-Ion battery systems, Boston: Boston: Artech House, 2015.

[34] Andreas Thingvad, Lisa Calearo, Peter Bach Andersen and Mattia Marinelli, "Empirical Capacity Measurements of Electric Vehicles Subject to Battery Degradation From V2G Services," *IEEE TRANSACTIONS ON VEHICULAR TECHNOLOGY,* vol. 70, no. 8, pp. 7547-7557, 2021.

## 8. Appendices

The MATLAB codes used to draw figure 6 is given below-

```
T_array = 273:373;
SOC_array = 0:1:100;
I_array = 0:0.1:10;

R_e = zeros(length(T_array), length(SOC_array), length(I_array));
Q_irrev = zeros(length(T_array), length(SOC_array), length(I_array));
for ii = 1:length(I_array)
    I = I_array(ii);
    for jj = 1:length(SOC_array)
        SOC = SOC_array(jj)/100;
        for kk = 1:length(T_array)
            T = T_array(kk);
            R_e(kk, jj, ii) = 27.54 - 27.68*exp(-1.91/T) + 223.71/(1 + 21.1*SOC) -
225.06*exp(-1.91/T)/(1 + 21.61*SOC);
            Q_irrev(kk, jj, ii) = I^2 * R_e(kk, jj, ii);
        end
    end
end

figure
for ii = 1:length(I_array)
    surf(SOC_array, T_array, squeeze(Q_irrev(:, :, ii)), 'LineStyle', 'none')
    hold on
end
xlabel('State of Charge (SOC)')
ylabel('Temperature (K)')
zlabel('Irreversible Heat (Q_{irrev})')
title('Irreversible Heat Generation as a function of SOC and Temperature');
```

The MATLAB codes used to draw figure 7 & 8 is given below-

```
% Constants
C_rate = 0.2;               % C-rate
capacity=2.2;

% Define the range of SOC values
SOC = 0.2:0.1:0.8;

% define current
I=capacity*C_rate;

% Calculate Qrev using the given equation
dUdT = 29.41 * SOC.^6 - 54.18 * SOC.^5 + 20.64 * SOC.^4 + 8.4946 * SOC.^3 - 5.4224 * SOC.^2 +
1.0674 * SOC - 0.205;

Qrev = I * dUdT;

% Plotting the results
```

```
plot(SOC, Qrev, 'o-')
xlabel('SOC')
ylabel('Q_{rev}')
title('Q_{rev} vs. SOC, +ve current')
grid on
```

The MATLAB codes used to draw figure 9 to 11 is given below-

```
% Constants
C_rates = linspace(0.1, 0.2, 10); % C-rates from 0.1C to 0.2C
capacity = 2.2;                % Capacity of the cell in Ah
T = 30;                    % Temperature in Kelvin
SOC = 0.4;                   % State of Charge
h = 3.25;                  % Heat transfer coefficient
A = 0.01;                  % Surface area in square meters
T_fluid = 25;                % Fluid temperature in Kelvin
epsilon = 0.02;              % Emissivity
sigma = 5.96e-8;               % Stefan-Boltzmann constant
T_a = 25;                  % Ambient temperature in Kelvin

% Function definitions for Re and dUdT
Re = @(T) 27.54 - 27.68 * exp(-1.91 / T) + 223.711 / (1 + 21.1 * SOC) - 225.06 * exp(-1.91 / T) / (1 +
21.61 * SOC);
dUdT = @(SOC) 29.41 * SOC.^6 - 54.18 * SOC.^5 + 20.64 * SOC.^4 + 8.4946 * SOC.^3 - 5.4224 *
SOC.^2 + 1.0674 * SOC - 0.205;

% Integration settings
t_start = 0;                % Start time in seconds
t_end = 300;                % End time in seconds
N = 300;                   % Number of intervals

% Time vector
t = linspace(t_start, t_end, N+1);

% Initialize total_heat matrix
total_heat = zeros(length(C_rates), N+1);

% Integrate the function for each C_rate
for j = 1:length(C_rates)
    C_rate = C_rates(j);

    % Define Current
    I = capacity * C_rate;

    % SOC vector
    SOC = linspace(0.8, 0.2, N+1);

    % Time step
    dt = (t_end - t_start) / N;

    % Initialize generated heat
    generated_heat = zeros(1, N+1);
```

```
    gen_heat = zeros(1, N+1);

    % Integrate the function
    for i = 1:N
        % Current time
        ti = t(i);

        % Next time
        ti_plus_1 = t(i+1);

        % Calculate Re at the current temperature
        Re_current = Re(T);

        % Calculate dUdT at the current SOC
        dUdT_current = dUdT(SOC(i));

        % Calculate the function value at the current time
        function_value = (I.^2 * Re_current) - (I * T * dUdT_current);
        function_values = (I.^2 * Re_current) + (I * T * dUdT_current);

        % Integrate the function using the trapezoidal rule
        generated_heat(i+1) = generated_heat(i) + 0.5 * (function_value + ((I.^2 * Re(T)) - (I * T *
dUdT(SOC(i))))) * dt;
        gen_heat(i+1) = gen_heat(i) + 0.5 * (function_values + ((I.^2 * Re(T)) + (I * T * dUdT(SOC(i))))) *
dt;
    end

    % Calculate total heat
    total_heat(j, :) = generated_heat + gen_heat;
end

% Plot the 3D graph
figure;
[X, Y] = meshgrid(t, C_rates);
surf(X, Y, total_heat);
xlabel('Time (s)');
ylabel('C-rate');
zlabel('Total Generated Heat (J)');
title('Total Generated Heat for Different C-rates');
```

The MATLAB codes used to draw figure 12 to 14 is given below-

```
% Constants
C_rate = linspace(0.1, 0.2, 100);  % C-rate range from 0.1C to 0.2C
capacity = 2.2;                % Capacity of the cell in Ah
T = 30;                      % Temperature in Kelvin
SOC = 0.4;                    % State of Charge
h = 3.25;                    % Heat transfer coefficient
A = 0.01;                    % Surface area in square meters
T_fluid = 25;                 % Fluid temperature in Kelvin
epsilon = 0.02;               % Emissivity
```

```
sigma = 5.96e-8;              % Stefan-Boltzmann constant
T_a = 25;                     % Ambient temperature in Kelvin

% Function definitions for Re and dUdT
Re = @(T) 27.54 - 27.68 * exp(-1.91 / T) + 223.711 / (1 + 21.1 * SOC) - 225.06 * exp(-1.91 / T) / (1 +
21.61 * SOC);
dUdT = @(SOC) 29.41 * SOC.^6 - 54.18 * SOC.^5 + 20.64 * SOC.^4 + 8.4946 * SOC.^3 - 5.4224 *
SOC.^2 + 1.0674 * SOC - 0.205;

% Function definition for the dissipated heat
dissipated_heat = @(T) h * A * (T - T_fluid) + epsilon * sigma * A * (T^4 - T_a^4);

% Integration settings
t_start = 0;                  % Start time in seconds
t_end = 1800;                 % End time in seconds
N = 1800;                     % Number of intervals

% Initialize accumulated heat matrix
accumulated_heat = zeros(length(C_rate), N+1);

% Integrate the function for each C-rate value
for i = 1:length(C_rate)
    % Define Current
    I = capacity * C_rate(i);

    % Time vector
    t = linspace(t_start, t_end, N+1);

    % SOC vector
    SOC = linspace(0.2, 0.8, N+1);

    % Time step
    dt = (t_end - t_start) / N;

    % Initialize generated heat
    generated_heat = zeros(1, N+1);
    gen_heat = zeros(1, N+1);
    total_heat = zeros(1, N+1);
    dissipated_heat_values = zeros(1, N+1);

    % Integrate the function
    for j = 1:N
        % Current time
        ti = t(j);

        % Next time
        ti_plus_1 = t(j+1);

        % Calculate Re at the current temperature
        Re_current = Re(T);
```

```
        % Calculate dUdT at the current SOC
        dUdT_current = dUdT(SOC(j));

        % Calculate the function value at the current time
        function_value = (I.^2 * Re_current) - (I * T * dUdT_current);
        function_values = (I.^2 * Re_current) + (I * T * dUdT_current);
        function_valuess = dissipated_heat(T);

        % Integrate the function using the trapezoidal rule
        generated_heat(j+1) = generated_heat(j) + 0.5 * (function_value + ((I.^2 * Re(T)) - (I * T *
dUdT(SOC(j))))) * dt;
        gen_heat(j+1) = gen_heat(j) + 0.5 * (function_values + ((I.^2 * Re(T)) + (I * T * dUdT(SOC(j))))) *
dt;
        total_heat(j+1) = generated_heat(j+1) + gen_heat(j+1);
        dissipated_heat_values(j+1) = dissipated_heat_values(j) + 0.5 * (function_valuess +
dissipated_heat(T)) * dt;
        accumulated_heat(i, j+1) = total_heat(end) - dissipated_heat_values(end);
    end
end

% Create a meshgrid for C-rate and time
[C_rate_mesh, t_mesh] = meshgrid(C_rate, t);

% Create the 3D plot
figure;
surf(C_rate_mesh, t_mesh, accumulated_heat');
xlabel('C-rate');
ylabel('Time (s)');
zlabel('Accumulated Heat (J)');
title('Accumulated Heat for diff C-rates in 30 minutes');
colorbar;

% Rotate the plot to view from different angles
view(45, 30);
```

The MATLAB codes used to draw figure 15 to 17 is given below-

```
% Constants
C_rates = linspace(0.09, 0.15, 10); % C-rates from 0.09C to 0.15C
capacity = 2.2;              % Capacity of the cell in Ah
T = 30;                      % Temperature in Kelvin
SOC = 0.4;                   % State of Charge
h = 3.25;                    % Heat transfer coefficient
A = 0.01;                    % Surface area in square meters
T_fluid = 25;                % Fluid temperature in Kelvin
epsilon = 0.02;              % Emissivity
sigma = 5.96e-8;             % Stefan-Boltzmann constant
T_a = 25;                    % Ambient temperature in Kelvin
V = 3.6;                     % Cell voltage in Volts

% Function definitions for Re
Re = @(T) 27.54 - 27.68 * exp(-1.91 / T) + 223.711 / (1 + 21.1 * SOC) - 225.06 * exp(-1.91 / T) / (1 +
```

```
21.61 * SOC);

% Function definition for the dissipated heat
dissipated_heat = @(T) h * A * (T - T_fluid) + epsilon * sigma * A * (T^4 - T_a^4);

% Integration settings
t_start = 0;                % Start time in seconds
t_end = 60;                 % End time in seconds
N = 60;                   % Number of intervals

% Initialize optimized_heat matrix
optimized_heat = zeros(length(C_rates), N+1);

% Integrate the function for each C_rate
for j = 1:length(C_rates)
    C_rate = C_rates(j);

    % Define Current
    I = capacity * C_rate;

    % Time vector
    t = linspace(t_start, t_end, N+1);

    % SOC vector
    SOC = linspace(0.8, 0.2, N+1);

    % Initialize generated heat
    generated_heat = zeros(1, N+1);
    dissipated_heat_values = zeros(1, N+1);

    % Integrate the function
    for i = 1:N
        % Current time
        ti = t(i);

        % Next time
        ti_plus_1 = t(i+1);

        % Calculate Re at the current temperature
        Re_current = Re(T);

        % Calculate the function value at the current time
        function_value = (I.^2 * Re_current) * dt;
        function_values = dissipated_heat(T);

        % Integrate the function using the trapezoidal rule
        generated_heat(i+1) = generated_heat(i) + 0.5 * (function_value + (I.^2 * Re_current) * dt);
        dissipated_heat_values(i+1) = dissipated_heat_values(i) + 0.5 * (function_values +
dissipated_heat(T)) * dt;

        % Calculate the optimized heat
```

```
        optimized_heat(j, i+1) = generated_heat(i+1) - dissipated_heat_values(i+1);
    end
end

% Plot the optimized heat for each C-rate
figure;
hold on;
for j = 1:length(C_rates)
    plot(t, optimized_heat(j, :), 'LineWidth', 1.5);
end

hold off;

% Customize the plot
xlabel('Time (s)');
ylabel('Optimized Heat (J)');
title('Optimized Heat for 1 minute');
grid on;

% Create a legend for the C-rates
legend(cellstr(num2str(C_rates', 'C-rate = %.2f')));

% Adjust the figure size for better visibility
fig = gcf;
fig.Position(3:4) = [800, 600];
```

The MATLAB codes used to draw figure 18 AND 19 is given below-

```
% Define the parameters and initial conditions
Q = 2.2;
R1 = 0.05;
R2 = 0.05;
Rs = 0.01;
C1 = 15; % capacitance of the first branch in microF
C2 = 10; % capacitance of the second branch in microF
lambda_1 = -1/(R1*C1);
lambda_2 = -1/(R2*C2);
SOC_0 = 0.1:0.1:1.0; % Vary SOC_0 from 0 to 1
V_ocv_setpt = 3.7;
delta_V_oc_delta_SOC = 0.2;
y_min = 2.5;
y_max = 4.2;
t_0 = 0;
delta_t = 0.1;
T = 100;

% Define the state matrix A, input matrix B, output matrix C, and feedthrough matrix D
A = [0 0 0; 0 lambda_1 0; 0 0 lambda_2];
B = [-1/Q; lambda_1*R1; lambda_2*R2];
C = [delta_V_oc_delta_SOC -1 -1];
D = Rs;
```

```
% Define the time vector t and the input vector I(t)
t = t_0:delta_t:T;
I = zeros(size(t));

% Define the state vector x and the output vector y
x = [SOC_0(1); 0; 0];
y = C*x + D*I(1) + V_ocv_setpt - delta_V_oc_delta_SOC*SOC_0(1);

% Define the range of limiting currents and temperatures
I_min_max = linspace(-10, 10, 100);
T_bat = linspace(0, 50, 100);

% Calculate the power limits for each combination of limiting current, temperature, and SOC_0
P_limit = zeros(length(I_min_max), length(T_bat), length(SOC_0));
for k = 1:length(SOC_0)
   for i = 1:length(I_min_max)
      for j = 1:length(T_bat)
         % Calculate the limiting current based on the desired output
         y_lim = 3.8; % Desired output value
         A_star = expm(A*delta_t);
         x_hat = [SOC_0(k); y - V_ocv_setpt + delta_V_oc_delta_SOC*SOC_0(k); y - V_ocv_setpt +
delta_V_oc_delta_SOC*SOC_0(k)];
         I_min_max_temp = inv(C*A_star*B + D)*(y_lim - V_ocv_setpt +
delta_V_oc_delta_SOC*SOC_0(k) - C*A_star*x_hat);

         % Check if the limiting current violates the thermal constraint
         if T_bat(j) < 15 || T_bat(j) > 35
            I_min_max_temp = 0;
         end

         % Calculate the power limit
         if I_min_max(i) < I_min_max_temp
            P_limit(i, j, k) = I_min_max(i) * (y_max - V_ocv_setpt + delta_V_oc_delta_SOC*SOC_0(k));
         else
            P_limit(i, j, k) = I_min_max_temp * (y_max - V_ocv_setpt +
delta_V_oc_delta_SOC*SOC_0(k));
         end
      end
   end
end

% Create separate figures for each SOC_0 value
for k = 1:length(SOC_0)
   figure;
   surf(I_min_max, T_bat, P_limit(:, :, k)');
   xlabel('Limiting Current (A)');
   ylabel('Cell Temperature (C)');
   zlabel('Power Limit (W)');
   title(['Power Limits vs Limiting Current and Temperature at SOC ' num2str(SOC_0(k))]);
   colorbar;
end
```